



## UvA-DARE (Digital Academic Repository)

### Going in the right direction

*Cellular mechanisms underlying root halotropism*

Korver, R.A.

#### Publication date

2019

#### Document Version

Other version

#### License

Other

[Link to publication](#)

#### Citation for published version (APA):

Korver, R. A. (2019). *Going in the right direction: Cellular mechanisms underlying root halotropism*. [Thesis, fully internal, Universiteit van Amsterdam].

#### General rights

It is not permitted to download or to forward/distribute the text or part of it without the consent of the author(s) and/or copyright holder(s), other than for strictly personal, individual use, unless the work is under an open content license (like Creative Commons).

#### Disclaimer/Complaints regulations

If you believe that digital publication of certain material infringes any of your rights or (privacy) interests, please let the Library know, stating your reasons. In case of a legitimate complaint, the Library will make the material inaccessible and/or remove it from the website. Please Ask the Library: <https://uba.uva.nl/en/contact>, or a letter to: Library of the University of Amsterdam, Secretariat, P.O. Box 19185, 1000 GD Amsterdam, The Netherlands. You will be contacted as soon as possible.

# Chapter 4

## **Arabidopsis PLD $\zeta$ 1 impacts root tropisms by modulating cellular localization of auxin transport carriers**

Ruud A. Korver<sup>1</sup>, Thea van den Berg<sup>3</sup>, Jessica Meyer<sup>1,2</sup>, Carlos S. Galvan-Ampudia<sup>1#</sup> Kirsten H. W. J. ten Tusscher<sup>3</sup> and Christa Testerink<sup>1,2</sup>

<sup>1</sup>Plant Cell Biology, Swammerdam Institute for Life Sciences, University of Amsterdam, The Netherlands

<sup>2</sup>Plant Physiology, Department Plantenwetenschappen, Wageningen University & Research, The Netherlands

<sup>3</sup>Theoretical Biology, Department of Biology, Utrecht University, 3584 CH Utrecht, The Netherlands

# current address: Laboratoire de Reproduction et Développement des Plantes, Université de Lyon, Ecole Normale Supérieure de Lyon, Université Claude Bernard Lyon 1, CNRS, INRA, F-69364 Lyon, France

## Abstract

Changes in the endocytosis and re-localization of auxin carriers represent an important mechanism for adapting plant growth- and developmental responses, especially upon experiencing salinity stress. Following their homology to mammalian phospholipase Ds (PLDs), the PLD $\zeta$ s in plants are likely candidates to regulate auxin-carrier endocytosis. *Arabidopsis thaliana* contains two PLD $\zeta$  isoforms, PLD $\zeta$ 1 and PLD $\zeta$ 2. While a role in halotropism and gravitropism has been reported for PLD $\zeta$ 2, the underlying cellular mechanisms still remain unclear, as does the potential involvement of PLD $\zeta$ 1. Here, tropic phenotypes in a *pld $\zeta$ 1*-KO mutant were investigated, together with the dynamics of two auxin transporters during salt stress, *i.e.* the efflux carrier, PIN2 and the influx carrier, AUX1. We found altered halotropic- and gravitropic responses in absence of PLD $\zeta$ 1, and report a role for PLD $\zeta$ 1 in the polar localization of PIN2, both under normal conditions and during salt stress. Irrespective of the genetic background, salt stress induced changes in AUX1 polarity. Based on our earlier model, we found that these novel salt induced-AUX1 changes contribute to halotropic auxin asymmetry. Our updated model predicts that the differences in salt induced-PIN2 changes in the *pld $\zeta$ 1* mutant indeed lead to slower build-up of auxin asymmetry. In this paper, we also describe the formation of so-called 'Osmotic Stress-Induced Structures' (OSIMS) that, to our knowledge, have not been described before. They represent large ( $\pm$  600 nm) membrane structures that are formed at the plasma membrane, shortly after NaCl or sorbitol treatment and remain present in a *pld $\zeta$ 1* mutant, while they disappear in the wildtype. OSIMS do not co-localize with clathrin and their formation is not altered when sterol-influencing drugs are applied during salt stress. Taken together, these results increase our knowledge on auxin carrier dynamics during salt stress.

## Introduction

Soil conditions are one of the major decisive factors whether particular crops can be cultivated. For example, water and nutrient availability, pH, salinity, heavy metals, but also the microbiome, all represent important factors influencing plant growth and survival (Berendsen et al., 2012; Kochian et al., 2015; Munns and Gilliam, 2015). Hence, drought, nutrient-poor soil or high-soil salinity are often the cause of soil degradation. As a result of climate change, these conditions are found more frequently and are more extreme. Consequently, the amount of arable land in the world is declining. On all continents, salt-affected soils are present, with the most in the Middle East, Oceania and North Africa with 189 Mha, 169 Mha and 144 Mha of affected land, respectively (Wicke et al., 2011). Moreover, moderate levels of soil salinity already cause a decrease in yield. Therefore, improving the salt tolerance of crops is important to secure our food supply in the coming future, where we face an increasing population and decreasing amount of arable land.

Roots in a saline soil have to cope with  $\text{Na}^+$ -toxicity and osmotic stress. Root growth changes inherent to these conditions include a short-term arrest of root growth, called the quiescence phase (Geng et al., 2013), after which growth recovers, though never reaches the same rate as before the stress (Geng et al., 2013; Julkowska and Testerink, 2015). Main root and lateral roots are affected differently by soil salinity, resulting in differences in overall root system architecture (RSA) compared to control conditions (Julkowska et al., 2014), of which the genetic and molecular mechanisms are starting to be unravelled (Julkowska et al., 2017). Root development is controlled by local auxin maxima and minima. The former inhibits cell elongation and regulates lateral root emergence, while the latter have been shown to regulate the transition from cell division to cell differentiation (Di Mambro et al., 2017). Auxin is also known to regulate its own carriers and thus locally enhancing auxin flow and regulating organ formation (Laskowski et al., 2008). Shoot derived-auxin transport to the root involves polar auxin transport (PAT), which is regulated by auxin carriers and represents the best-studied processes of auxin-regulated growth and development (Armengot et al., 2016; Naramoto, 2017). Internalization of auxin carriers during recycling is dependent on clathrin-mediated endocytosis (Adamowski and Friml, 2015). Salt stress also induces endocytosis and while CME is often also proposed as the endocytotic pathway involved in the internalization of auxin carriers during salt stress, recent studies provide evidence for the involvement of clathrin-independent endocytosis (Titapiwatanakun et al., 2009; Baral et al., 2015).

Besides adaptation of overall RSA to saline soil, plants are also capable of changing their direction of root growth, i.e. away from salt, a phenomenon called halotropism (Galvan-Ampudia et al., 2013). During the halotropic response, a salt-induced increase in internalization and relocation of the auxin transporter, PIN2, on the salt-exposed side, changes the flow of auxin, causing an elevation of auxin levels on the non-exposed side of the root, inhibiting cell elongation. The net result is that the root bends away from the salt gradient (Galvan-Ampudia et al., 2013). Through a combination of computational modelling and *in planta* experiments, it was demonstrated that the internalization of only PIN2 would be insufficient to generate an effective auxin asymmetry (van den Berg et al., 2016). Up-regulation of AUX1 on the non salt-exposed side of the root, through a positive-feedback loop from an increasing auxin concentration was required to reach an auxin concentration that was sufficient to inhibit cell elongation. In addition, a transient increase of PIN1 in the stele was found to be essential (van den Berg et al., 2016).

Galvan-Ampudia *et al.* (2013) proposed that Phospholipase D zeta 2 (PLD $\zeta$ 2) was involved in an increase in CME of PIN2 during salt stress. Arabidopsis has a total of 12 PLDs, including two PLD $\zeta$ s. The PLD $\zeta$ 's stand out from the other 10 plant PLD's, as they lack a Ca<sup>2+</sup>-dependent C2-binding domain, making them Ca<sup>2+</sup> independent. Instead, they contain a pleckstrin homology (PH) domain and a Phox (PX) domain, which bind phosphatidylinositol lipids in membranes. Nevertheless, this has never been shown for the plant PLD $\zeta$ s. Up to date, not much is known about the role of PLD $\zeta$ s in endocytosis. However, much can be learned from mammalian systems. The two PLDs of mammalian systems; PLD1 and PLD2 have been linked to endocytosis (Donaldson, 2009). Of the plant PLDs, the PLD $\zeta$ s are most homologous to the mammalian PLD1 and PLD2 (Qin and Wang, 2002), suggesting plant PLD $\zeta$ 's could play a role in endocytosis. For PLD $\zeta$ 2 involvement during halotropism (Galvan-Ampudia et al., 2013), gravitropism (Li and Xue, 2007) and hydrotropism (Taniguchi et al., 2010) has been shown.

PLDs hydrolyze structural phospholipids, like phosphatidylcholine (PC) to produce phosphatidic acid (PA) that can function as lipid second messenger (for reviews, see (Munnik, 2001; McDermott et al., 2004)). For example, PA acts as a signal for cytosolic proteins to be recruited to the PM (Testerink and Munnik, 2011). In addition, due to its small headgroup, PA also increases the negative curvature at the cytoplasmic leaflet of membranes thereby facilitating membrane fusion and -fission by (Kooijman et al., 2003; Testerink and Munnik, 2011; Yao and Xue, 2018). In mammalian cells, PLD2 had been implicated in

clathrin-mediated endocytosis (Du et al., 2004) and caveolae-mediated endocytosis (Jiang et al., 2016).

In plants, an increase in PLD-generated PA have been reported in response to water deficit (Jacob et al., 1999; Frank et al., 2000) and during osmotic- and salt stress (Munnik et al., 2000). For Arabidopsis, genetic evidence for the involvement of PLD $\alpha$ 1 and PLD $\delta$  in salt stress has been shown (Bargmann et al., 2009). Meanwhile, several candidate PA-binding proteins have been found in the peripheral membrane fraction of salt-stressed roots (McLoughlin et al., 2013).

An increase in CME during salt stress is potentially the pathway for internalization of PIN2 during halotropism. Treatment with an inhibitor of mammalian PLDs, FIPI (5-Fluoro-2-indolyl des-chlorohalopemide) (Su et al., 2009), hampered clathrin localization to the membrane (Galvan-Ampudia et al., 2013). Subsequently, PIN2 localization during salt treatment was altered in presence of FIPI. However, *pld $\zeta$ 2* mutants only exhibited a weak halotropic response, indicating the involvement of other PLDs. Next to the putative involvement in PIN2 endocytosis during salt stress, as mentioned above, knowledge on plant PLDs and their role in endocytosis is scarce (Pleskot et al., 2012; Takac et al., 2012).

So far, a role for PLD $\zeta$ 1 in salt stress and tropism responses have remained elusive. Inducible RNAi inhibition of PLD $\zeta$ 1 resulted in deformed root hairs and an altered root hair patterning (Ohashi et al., 2003). Similarly, involvement of PLD $\zeta$ 1 in root development during phosphate starvation has been described (Li et al., 2006). Under phosphate limiting conditions, the *pld $\zeta$ 1/pld $\zeta$ 2*-double mutant, but not the single mutants, exhibited shorter main roots and longer lateral roots.

We set out to investigate a putative role for PLD $\zeta$ 1 in salt stress and especially in halotropism. We hypothesized that PLD $\zeta$ 1 is involved in tropism responses as a result of its homology to PLD $\zeta$ 2 and mammalian PLD's. Therefore, we investigated root growth direction of a *pld $\zeta$ 1* mutant using both halotropism and gravitropism assays. In addition, we studied auxin carrier localization during salt stress in a *pld $\zeta$ 1* mutant.

## Results

### PLD $\zeta$ 1 is involved in altering the root-growth direction during tropisms

To assess the putative role of PLD $\zeta$ 1 during halotropism, roots from a *pld $\zeta$ 1*-KO mutant were followed for one day on vertical agar plates, containing either control medium or a salt gradient produced by 200 mM NaCl (Galvan-Ampudia

et al., 2013). On control plates, *pldζ1* seedlings were found to display a stronger skewing effect to the right than wild type (Supplemental figure S1a-b). On salt, the *pldζ1* seedlings exhibited a slower halotropism response and they did not reach the same angle of bending as the wildtype within 24 h (Figure 1a-b). During the long-term halotropic response, no difference between wild type and *pldζ1* was found until day 4, where even a slightly larger angle away from the salt gradient was observed (Supplemental figure S1c). To determine whether *pldζ1* roots were also impaired in the gravitropic response, seedlings were grown on vertical agar plates and the root-growth direction monitored after changing the plates by 90°. Surprisingly, *pldζ1* roots were found to display an exaggerated gravitropic response compared to the wild type (Figure 2a-b). While wild-type roots remained at an angle of about 10° 5 hrs after reorientation, the *pldζ1* roots kept bending towards gravity. The difference was found up to 7 hrs after reorientation. Skewing during normal growth was not seen until 15h after re-orientation of the plate (Figure 2b). The slower halotropic response and the exaggerated gravitropic response were both rescued by expression of

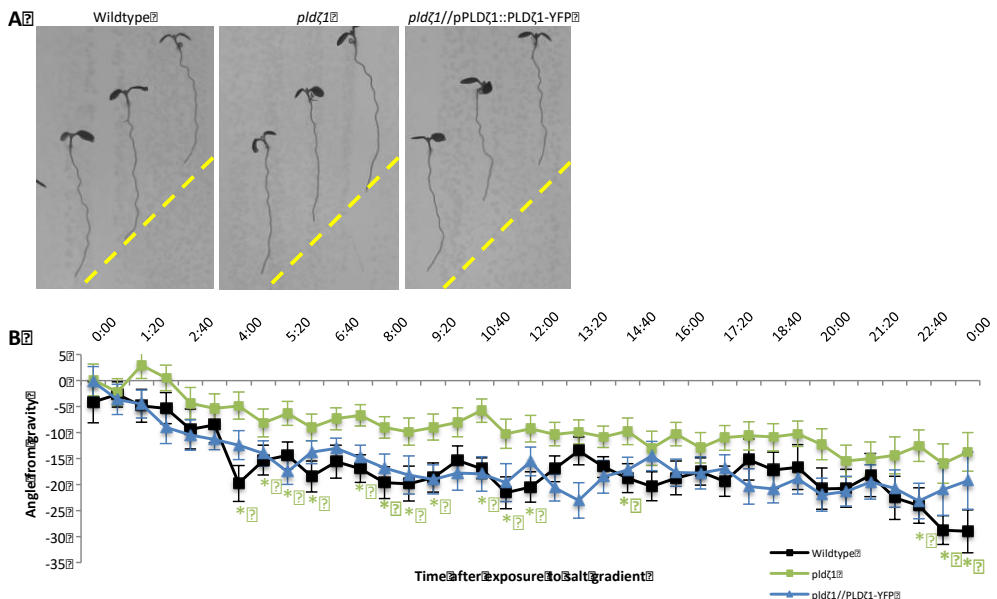


**Figure 1: *pldζ1* mutant plant roots show a delayed halotropism response.** (A) Representative images of WT (Col-0), *pldζ1* and *pldζ1//pPLDζ1::PLDζ1-YFP* seedlings 24 hours after exposure to a 200 mM NaCl gradient in a time-lapse set-up. Yellow dashed lines show start of gradient. (B) Quantification of the growth angle over the first 24 hrs after exposure to the 200mM salt gradient. (combined data of 2 biological replicas, WT n=34, *pldζ1* n=38, *pldζ1//pPLDζ1::PLDζ1-YFP* n=32). Asterisks show significant differences (p<0.05 in a univariate ANOVA, Tukey post hoc), the color of the asterisks correspond to the line with a significant difference from wildtype.

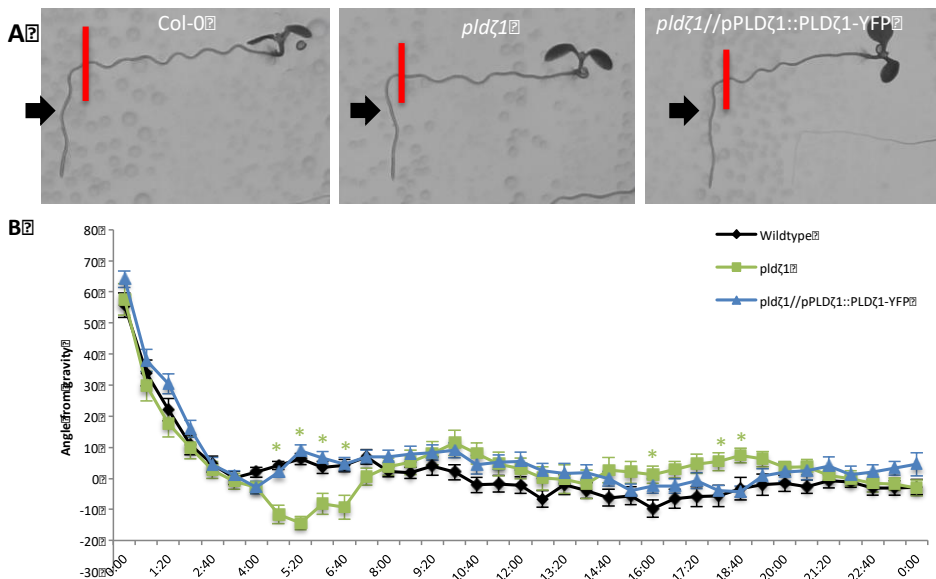


**Figure 2: *pldζ1* roots show an exaggerated gravitropic response.** (A) Representative images of WT (Col-0), *pldζ1* and *pldζ1//pPLDζ1::PLDζ1-YFP* seedlings 24 hours after a 90 degrees reorientation. Red bars show the position of the root tip immediately after reorientation. Black arrows points at the 4:00 timepoint. (B) Quantification of root growth angle over 24 hours after 90 degree re-orientation (2 biological replicates: WT n=22 , *pldζ1* n=24, *pldζ1//pPLDζ1::PLDζ1-YFP* n=30). Asterisks show significant differences ( $p < 0.05$  in a univariate ANOVA, Tukey post hoc), the color of the asterisks correspond to the line with a significant difference from wildtype.

*pPLDζ1::PLDζ1-YFP* in the *pldζ1*-mutant background (Figures 1a-b and 2a-b). In conclusion, PLDζ1 is involved in both the halotropic- and gravitropic response.

### AUX1 is internalized from the lateral side of the PM during salt stress

Our earlier work demonstrated the importance of the interplay between auxin-influx and -efflux carriers during halotropism (van den Berg et al., 2016). In the absence of auxin-induced changes in AUX1 expression would be insufficient to cause an auxin asymmetry. To determine the cellular dynamics of AUX1 during salt stress, we imaged AUX1-mVenus during control- and salt treatments over time. As expected, AUX1 showed a less polar distribution than PIN2-GFP in control conditions (Band et al., 2014), which was similar for wildtype and *pldζ1* roots (Figure 3a,b). After 5 min of 120 mM NaCl, AUX1 was observed to cluster in what appeared to be domains of about 300 nm in the PM. In wildtype plants, this clustering occurred simultaneously with a decrease of the combined apical and basal signal (apical/basal component), while its lateral abundance did not change. In contrast, in *pldζ1* plants, most lateral rather than apical/basal AUX1 abundance decreased (Figure 3b). After 60 min of salt treatment, the

apical/basal AUX1-mVenus signal recovered to mock treatment levels for both wildtype and *pldζ1*, while the lateral signal decreased, the intracellular signal increased, and less clustering at the PM was found (Figure 3c). These results suggest an involvement of PLDζ1 in the early salt-induced AUX1 re-localization, not in the long term AUX1 response.

### **Modeling shows how salt-induced changes in AUX1 patterning contribute to root halotropism**

To investigate the effects of the altered AUX1 patterning during salt stress on halotropic auxin asymmetry, an updated version of our previously developed computational model for halotropism was used (van den Berg et al., 2016). Our experimental data indicated that after 60 min, roots showed restored apical/basal AUX1 levels and approximately a 20% reduction in lateral AUX1 levels. Therefore, simulations were run with the addition of this 20% reduction of AUX1. Interestingly, this gave rise to a 10%-elevated increase in auxin at the non-salt exposed side of the root (Figure 3d), while an even larger change in auxin decrease at the salt-exposed side occurred. Additionally, auxin re-routing occurred in a shorter time frame, while the rerouting also extended further shootward (Figure 3e). Remarkably, halotropism simulation with the 20% reduction of lateral AUX1 led to a larger increase of auxin concentration on the non salt-exposed side of the root in *pldζ1* compared to wildtype (Supplemental figure S2).

### **The PIN2 auxin efflux carrier is more apolarly distributed in a *pldζ1* line**

Next to the influx carrier AUX1, the efflux carrier PIN2 has also been reported to be affected by salt (Galvan-Ampudia et al., 2013). Hence, we investigated differences in the sub-cellular localization of PIN2 in root epidermal cells between wild-type and *pldζ1* with and without salt in the root elongation zone. Under control conditions, *pldζ1* mutants exhibited a more apolar distribution of PIN2-GFP compared to wild-type roots, with more PIN2 at the lateral-, and less at the apical membranes (Figure 4a-b). In salt-stressed wildtype, apical-PIN2 abundance decreased compared to total PIN2, while lateral- and intracellular-PIN2 abundance increased after at least 30 min (figure 4d), which was in accordance to earlier work (Galvan-Ampudia et al., 2013). Investigating earlier responses, we already found a PIN2 decrease at both apical- and lateral side of the membrane after 5 min, while the intracellular pool increased (Figure 4c). Thus, while initially all PIN2 at the membrane appears to decrease, at later stages PIN2 is re-localised to the lateral membrane. In contrast, a membrane protein unrelated to auxin transport, i.e. Plasma Membrane Proton ATPase 2

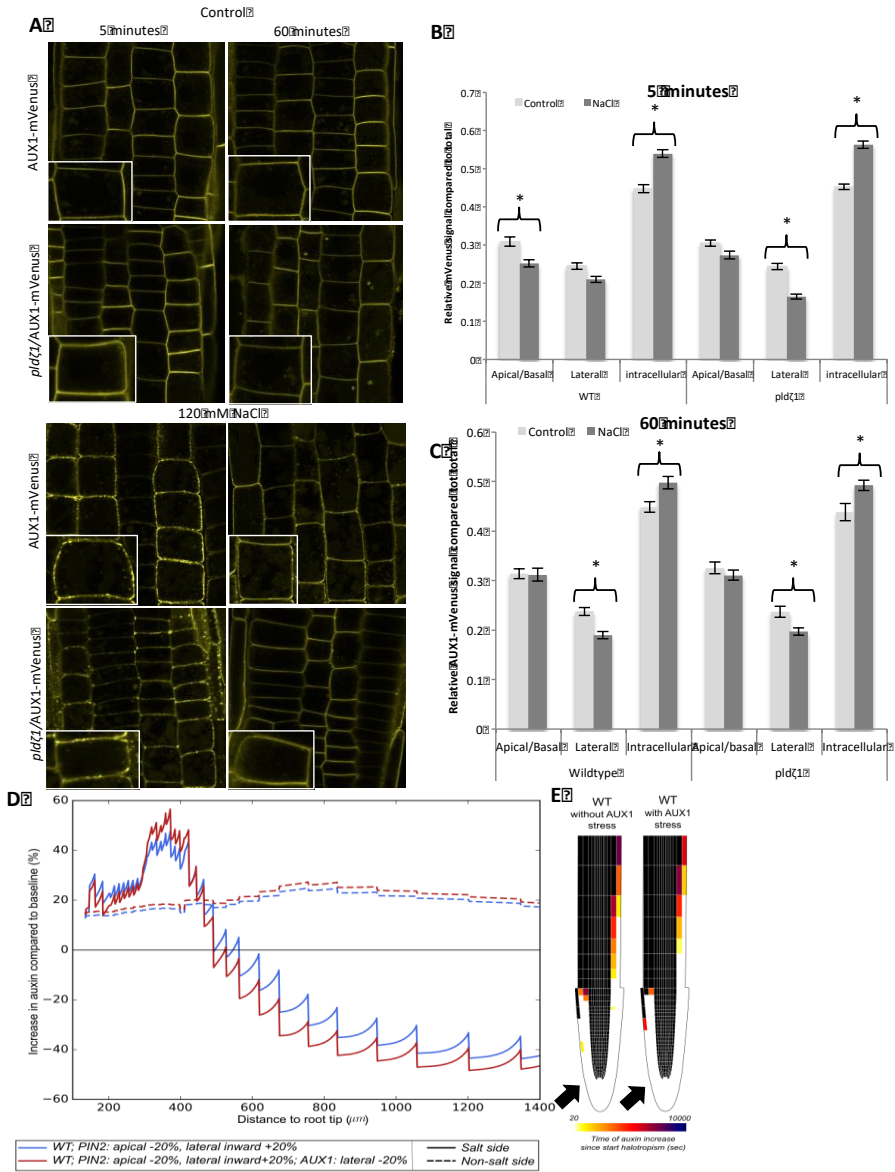


**Figure 3: After short-term differences in AUX1 dynamics between wildtype and *pldζ* during salt stress, cells show less AUX1 on the lateral side of the PM upon salt stress after 60 minutes.** (A) Representative pictures of AUX1-mVenus in wildtype and *pldζ1* background during control and salt stressed conditions. (B) Relative AUX1-mVenus signal abundance at the different sides of the PM compared to total signal in control and salt stress conditions after 5 minutes of treatment. Apical/basal is the combined signal of the adjacent apical and basal membrane because they are indistinguishable. (N is respectively 88, 80, 88 and 80 cells for Wt control, WT salt, *pldζ1* control and *pldζ1* salt). Asterisks show significant differences between control and salt ( $p < 0.05$  using *t*-test in SPSS 24) (C) Relative AUX1-mVenus signal abundance at the different sides of the PM compared to total signal in control and salt stress conditions after 60 minutes of treatment. (N is respectively 88, 64, 96 and 80 cells for Wt control, WT salt, *pldζ1* control and *pldζ1* salt). Asterisks show significant differences between control and salt ( $p < 0.05$  using *t*-test in SPSS 24) (D) Percentage change in epidermal auxin levels at the salt and non-salt exposed side of the root as a function of (continued below)

(PMA2), displayed no such polarity change (Supplemental figure S3). The *pldζ1* mutant showed similar changes to wildtype in cellular PIN2 patterning after 5 min salt stress (Figure 4c), but showed no additional re-localization of PIN2 to the lateral membrane at later stages (Figure 4d).

Next, we investigated whether the differences in PIN2 polarity during NaCl treatment were salt specific or caused by osmotic shock. In order to answer this question, roots were treated with an equal osmolality of sorbitol (240 mM), and the polarity of PIN2 determined after 5 and 30 min. Similar to 120 mM NaCl, the apical component of the PIN2-GFP signal in wild-type root epidermal cells decreased after 5 min (Figure 4c). The abundance of PIN2 at the lateral sides of the membrane, however, did not change while the intracellular signal increased. After 30 min, the apical-, lateral- and intracellular signals all remained at the same level as the 5 min sorbitol treatment. Thus, no significant PIN2 re-localization to the lateral sides of the PM in case of osmotic stress treatment was observed. No differences were found between the *pldζ1* mutant and wildtype with regard to PIN2 internalization and re-localization with sorbitol (Figure 4d). These results indicate that the observed PIN2 re-localization to the lateral sides of the PM upon salt stress is salt-specific.

### **Modeling demonstrates how differences in salt-induced PIN2 response delays root halotropism**

Because our experimental results showed that next to salt-induced changes in PIN2 polarity also the baseline PIN2 pattern differed between wildtype and the *pldζ1* mutant roots, we investigated whether the observed differences in basal-PIN2 patterning and those induced by salt could explain the observed response differences during halotropism. To simulate auxin patterning in the *pldζ1* mutant, we first applied the somewhat less-polarized *pldζ1* mutant baseline-PIN2 pattern in all lateral root cap- and epidermal cells at both sides of our 2D root tip model (wild type-apical PIN2: lateral PIN2 ratio = 1:0.1; *pldζ1*-apical PIN2: lateral PIN2 ratio = 0.85:0.11; based on Figure 4b). We tested whether our model would predict differences in epidermal auxin levels in control conditions due to these changes. Apart from modestly elevated auxin levels between 250 and 500 μm from the root tip, overall root auxin patterning was largely

**Figure 3 continued:** distance from the root tip for simulated halotropism in wildtype roots, thus a 20% reduction in apical PIN2 and a 20% increase in lateral PIN2 in the root epidermal and root cap cells on the salt-exposed side of the root. Changes were shown both for a situation not incorporating and a situation incorporating salt-induced AUX1 changes. Changes in auxin levels were shown for a timepoint 3 hrs after the start of halotropism. (E) Halotropism induced rerouting of auxin in the two corresponding situations. Rerouting is shown if cells experience a 10% or more increase in auxin, color coding indicates the time after start of halotropism when this rise in auxin levels occurs. Black arrows show the direction of the salt gradient.

unaffected (Supplemental figure S4). To simulate auxin patterning during halotropism in the *pldζ1* mutant, we applied the altered *pldζ1* type PIN2 salt responses in the higher lateral root cap- and epidermal cells of only the salt exposed side of the root. Based on our data (Figure 4c) we applied a smaller reduction in apical PIN2 levels and no increase in lateral PIN2 levels as compared to wild-type halotropism (wild-type halotropism = apical PIN2: lateral PIN2 ratio = 0.8:0.12; *pldζ1* halotropism = apical PIN2: lateral PIN2 ratio = 0.775:0.11). The model also included the salt-induced transient increase of PIN1, which was shown to be important for auxin asymmetry timing, and the auxin-induced expression of AUX1, important for auxin asymmetry amplification found earlier (van den Berg et al., 2016). Consistent with the experimentally-observed slower halotropic response, the model predicted that *pldζ1* has a slower, less distal rerouting of auxin to the non-salt exposed side of the root, and achieves substantially-less pronounced auxin asymmetry levels (18% vs 27% increase at the non-salt exposed side, and 17% vs 54% decrease at the salt-exposed side; Figure 4e and Supplemental figure S5d). Interestingly, we found that the salt-induced changes in AUX1 have a more pronounced auxin asymmetry-enhancing effect in the *pldζ1* mutant compared to wild type. These findings underline the importance of the newly found salt induced-AUX1 response for halotropism robustness.

Making use of the freedom that a mathematical model offers in separating and combining conditions not easily created *in planta*, we then decided to investigate to what extent differences in *pldζ1*-halotropism response depend on differences in basal PIN2 patterns and differences in salt induced-PIN2 responses. First, we investigated the effect of the differences in baseline conditions. For this, we combined the *pldζ1*-type of salt-induced PIN2 changes with different baseline conditions: wildtype, *pldζ1* or hybrid combinations (Supplemental figure S5a). Differences in baseline PIN2 patterns appear to have a small effect on the auxin increase at the non-salt exposed side, a somewhat larger effect on the auxin decrease on the salt-exposed side, as well as a small effect on the timing of auxin rerouting (Supplemental Figure 5b). The slightly larger asymmetry and rerouting speed arising in wild type as compared to *pldζ1* baseline-PIN2 conditions are predominantly caused by the difference in baseline apical PIN2 levels (Supplemental figure S4a). Next, we combined *pldζ1* baseline-PIN2 settings with different salt induced-PIN2 changes: wildtype, *pldζ1* or hybrid combinations. We find that it is predominantly the increase in lateral PIN2 levels occurring under salt in the wildtype but not *pldζ1*, that is critical for both the level of auxin asymmetry (Figure 4f, Supplemental figure S5c). The higher salt-induced apical-PIN2 levels in wild type relative to *pldζ1*

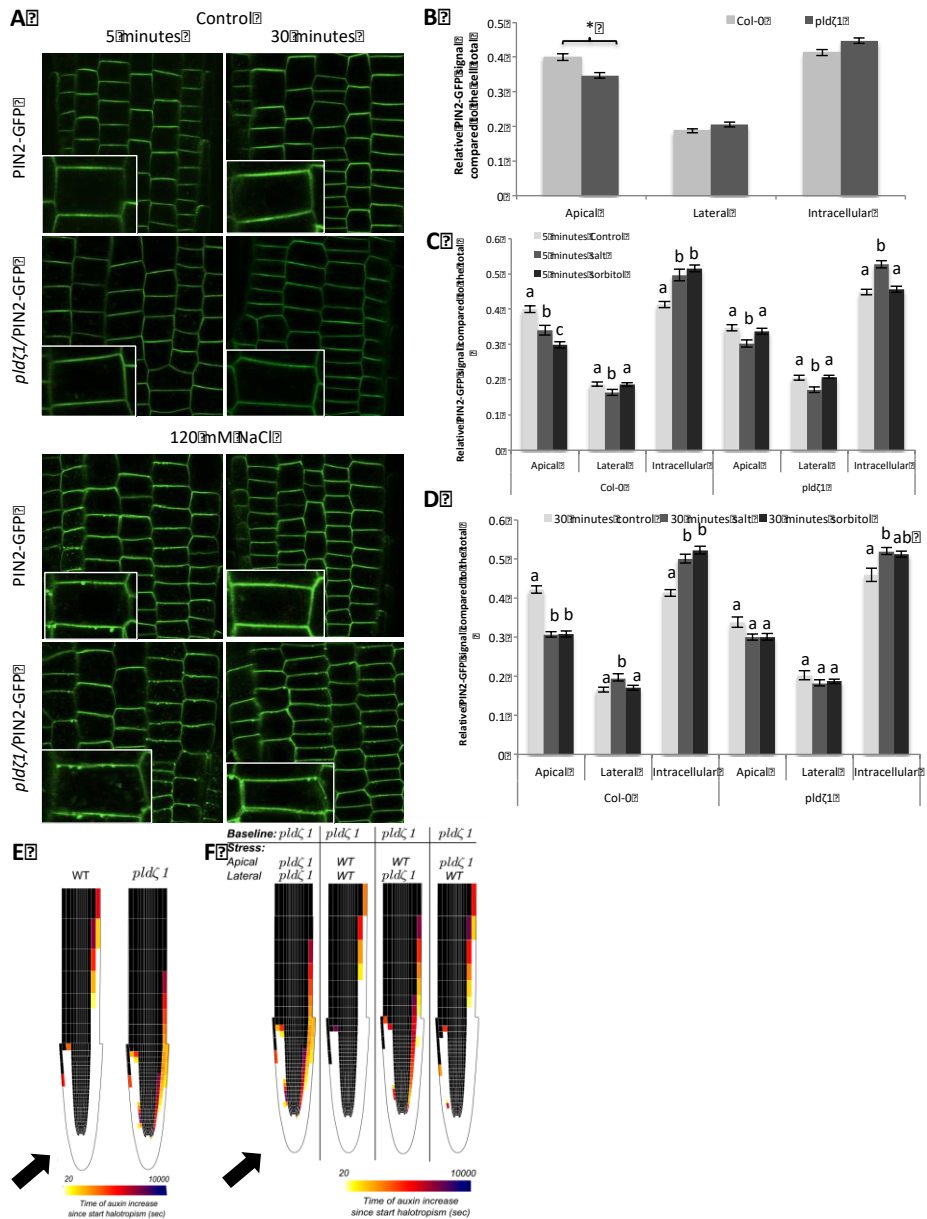


**Figure 4: Loss of PLD $\zeta$ 1 results in a more apolar PIN2 distribution and altered PIN2 re-localization upon salt stress.** Using a PIN2-GFP fusion protein in both wildtype (Col-0) and *pld $\zeta$ 1* background the intensity of the GFP signal on the apical and lateral sides of the membrane was measured next to the intracellular signal. (A) Representative images showing PIN2-GFP in WT and *pld $\zeta$ 1* in control and salt stress conditions after 5 and 60 minutes. (B) Quantification of PIN2-GFP signal intensity on the apical and lateral sides of the membrane and the intracellular signal intensity in control conditions in WT and *pld $\zeta$ 1*. Asterisks show significant differences between WT and *pld $\zeta$ 1* ( $p < 0.05$  in a univariate ANOVA, Tukey post hoc) (3 biological replicates,  $n = 96$  cells from 12 roots). (C) Quantification of PIN2-GFP signal at the different cell compartments after 5 minutes of control, salt or sorbitol treatment. Letters show significance groups between different treatments in either WT or *pld $\zeta$ 1* in one timepoint ( $p < 0.05$  in a univariate ANOVA, Tukey post hoc). (3 biological replicates,  $n > 80$ , from 10 roots or more). (D) Quantification of PIN2-GFP signal at the different cell (continued below)

only plays a minor role in both location and timing of the auxin asymmetry. These findings are consistent with our previous work, demonstrating the importance of lateral increased-PIN2 levels (van den Berg et al., 2016).

In conclusion, while the baseline-PIN2 differences cause a mild-slowness down and reduction of auxin rerouting during halotropism in the *pldζ1* mutant, it is predominantly the difference in salt induced-PIN2 localization changes relative to wild type that cause a slower halotropic response due to slower, less-spatially extended but foremost reduced auxin rerouting.

### NaCl and Sorbitol induce large membrane structures at the PM in epidermal en lateral root cap cells

Within 5 min after exposure of roots to NaCl or sorbitol, root cap and epidermal cells in wildtype roots were observed to form large, globular structures at the plasma membrane (Figure 4a). With a size of ~600 nm (Figure 5b), these structures are too large to be any known type of plasma membrane associated vesicle (Heuser, 1980; Homann, 1998). In wild-type seedlings, the number of these osmotic stress-induced membrane structures (from now on abbreviated to OSIMS) dramatically decreased after 15 min of stress treatment (Figure 5a), together with a small decrease in size, and after 60 min almost all OSIMS were gone. In contrast, the OSIMS in *pldζ1* roots build-up over a much longer time (up to 15 min), and still half of the OSIMSs remained present after 60 min of salt stress. In addition to these differences in temporal dynamics, also the sub-cellular localization of OSIMS showed a different pattern between wild type and *pldζ1* (figure 5c). In wild type, ~55% of the OSIMS were located at the apical side of the membrane, while ~35% resided in the corner region (undistinguishable whether it is located on the lateral or apical side) after 5 min salt stress. In *pldζ1* cells less OSIMS were found at the apical side of the membrane (~45%) and more at the corners (~45%). Besides, in *pldζ1* cells, this spatial distribution did not differ between different time points, yet in wild-type cells, even more OSIMS were found at the apical side (~64%) after 15 min of salt stress.

**Figure 4 continued:** compartments after 30 minutes of control, salt or sorbitol treatment. Letters show significance groups between different treatments in either WT or *pldζ1* in one timepoint ( $p < 0.05$  in a univariate ANOVA, Tukey post hoc) (3 biological replicates,  $n > 80$  from 10 roots or more). (E) Heatmaps showing halotropism induced auxin rerouting for wildtype and *pldζ1* settings. When a cell changes from black to colored, this indicates a auxin increase of at least 10%. The color indicates the timing of the auxin increase with lighter colors for short time periods. Black arrow indicates direction of the salt gradient (F) Changes in auxin rerouting for the different stress settings in the *pldζ1* mutant. The apical or lateral distribution of PIN2 using either the *pldζ1* settings or the wild type stress settings in the model is indicated. When a cell changes from black to colored, this indicates an auxin increase of at least 10%. The color indicates the timing of the auxin increase with lighter colors for short time periods. Black arrow indicates direction of the salt gradient.

Next, we used roots expressing AUX1-mVenus to determine if other, apolar auxin carriers were also located to OSIMS. Indeed they were, and no significant difference in the number of fluorescent OSIMS per cell was found between PIN2-GFP- and AUX1-mVenus-expressing epidermal root cells (Figure 5d,e). Following this result, we also found that PMA2-GFP appeared in OSIMS shortly after salt application (Figure 5d,e). Moreover, no significant difference in the number of OSIMS between PMA2- or PIN2-GFP-expressing lines was found 5 min after salt stress (Figure 5d). Imaging PIN2-GFP after treatment with 240 mM sorbitol also revealed OSIMS (Supplemental figure S6a) and no significant difference in the number of OSIMS were observed compared to salt. Similar to salt stress, these OSIMS were rarely observed after 60 min of sorbitol treatment (Supplemental figure S6b).

To test whether these OSIMS are larger forms of known endosomal structures, co-localization experiments with PIN2 and known endosomal markers were performed in wildtype and *pldζ1* background. These include RabF2b-RFP (ARA7) for multivesicular bodies, SYP32-RFP for the golgi network, RabA1e-RFP for recycling endosomes and VHA1-RFP for early endosomes (Dettmer et al., 2006; Geldner et al., 2009). However, none of the markers showed any co-localization with the PIN2-containing OSIMS after 5 min of NaCl treatment (Supplemental figure S7).

### **OSIMS do not co-localize with clathrin**

If OSIMS represent excess membrane material, the styryl dye FM4-64, used to label PM, should co-localize with the PIN2-GFP found in the OSIMS. Hence, Arabidopsis seedlings expressing PIN2-GFP were stained with FM4-64 (Figure 6e-f). PIN2-GFP and FM4-64 were found to co-localize, indicating that OSIMS are indeed membranous.

To investigate whether the OSIMS are part of an endocytic pathway, we tested whether OSIMS were associated with clathrin (CME) or whether the number of OSIMS would be decreased by pharmacological drugs that inhibit Membrane Microdomain-associated endocytosis (MMAE). For clathrin, we used a PIN2-GFP x CLC-mCherry line to image the subcellular localization of both proteins during early salt stress responses, and as shown in Figure 6a-b, no clathrin was found to associate with OSIMS. For the MMAE, two inhibitors were tested, i.e. methyl- $\beta$ -cyclodextrin and filipin (Ovecka et al., 2010; Valitova et al., 2014). However, neither affected the formation of OSIMS (Figure 6c-d) and no co-localization was found with the fluorescent filipin (Figure 9c-e). Together, these results suggest that OSIMS represent excess membrane material but not enlarged Clathrin-coated vesicles or internalized microdomains.

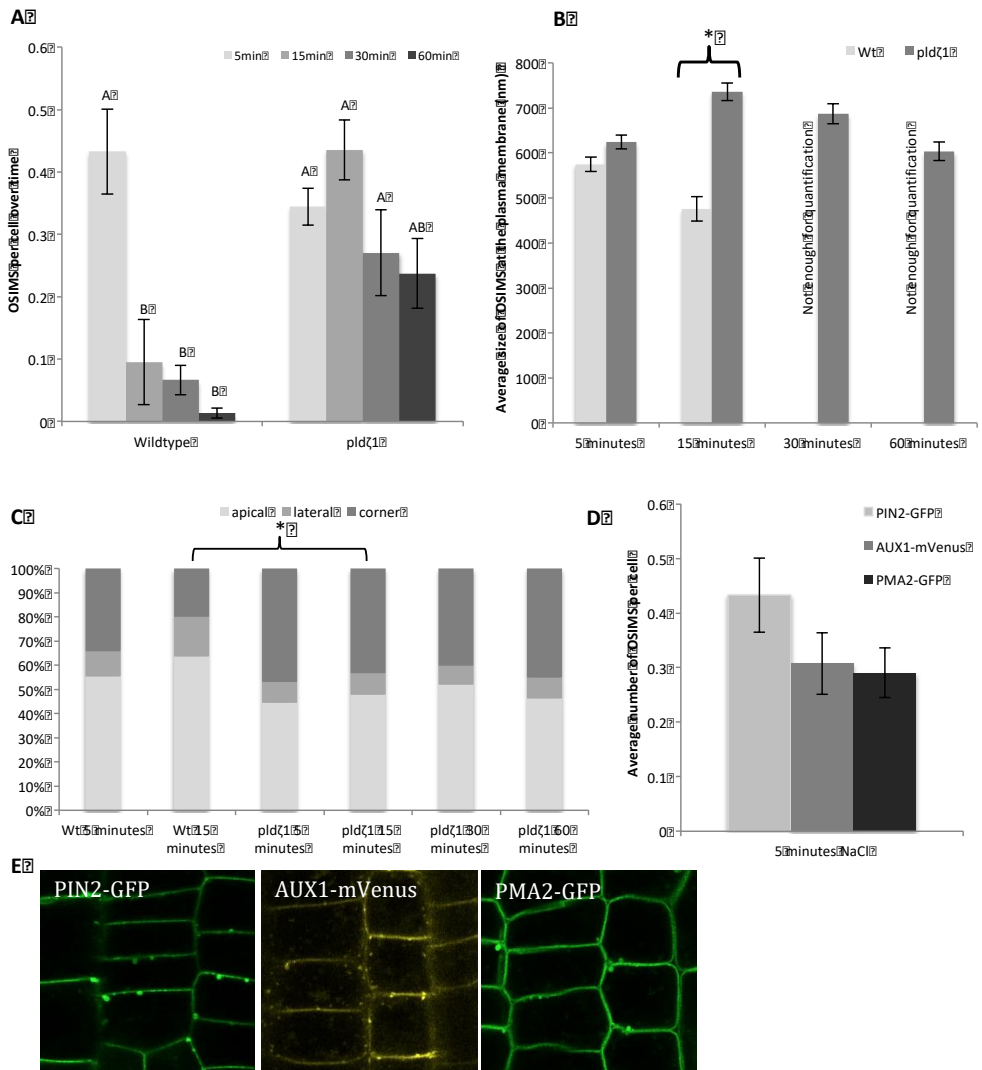


**Figure 5: *pld1* mutant plants have delayed processing of OSIMS at the plasma membrane.** (A) Quantification of amount of osmotic stress-induced membrane structures, OSIMS, at the plasma membrane in WT and *pld1* mutant plant epidermal cells in the lower elongation zone after 5, 15, 30 and 60 minutes (data is 3 biological replicates combined, n= between 350-500 cells per timepoint). (B) Average structure size in WT and *pld1* mutant plant epidermal cells in the lower elongation zone. Letters show significance groups,  $p < 0.05$  in a univariate ANOVA, Tukey post hoc in SPSS 24 (data is 3 biological replicates combined, n=50 for Col-0 15 minutes, for Col-0 5 minutes and all *pld1* n is between 150-250. For Col-0 30 and 60 minutes N<10 and they were not quantified). Asterisks show significant difference between Col-0 and *pld1*.  $p < 0.05$  in a *t*-test using SPSS 24 (C) Sub-cellular localization of the NaCl and Sorbitol induced structures at the plasma membrane. Structures scored as localized in the corner could not be scored as either apical or lateral (The same images were used for both size and location and the n is the same). Asterisks show significant differences between Wt and *pld1* for a timepoint ( $p < 0.05$  using a chi-square test in SPSS 24). (D) Comparison of the amount of OSIMS in a PIN2-GFP, AUX1-mVenus and PMA2-GFP line after 5 minutes of a 120mM salt stress. No significant differences were found using a univariate ANOVA with Tukey post hoc in SPSS 24. (E) Representative images of OSIMS in Arabidopsis roots expressing PIN2-GFP, AUX1-mVenus and PMA2-GFP after a 5 minute 120mM NaCl treatment.

### **OSIMS are processed slower in *pldζ1* roots**

The average number of OSIMS after 5 min of 120 mM NaCl or 240 mM sorbitol treatment in *pldζ1* epidermal-root cells did not differ significantly from those in wild type (Figure 5a). Interestingly, however, more OSIMS were observed in *pldζ1* roots after 60 min compared to wild type, in which most OSIMS had already disappeared. The average size increase to 700 nm after 15 min in the *pldζ1* roots also contrasts with the decrease in size in the wild-type roots during that same period (Figure 5b). The subcellular localization of OSIMS upon 120 mM NaCl treatment was mainly at the apical side of the plasma membrane with a few OSIMS at the lateral sides and about 25% in the corners of the cell (in which distinction between lateral- and apical was impossible to make). This corresponds well with the large decrease in apical PIN2 localization during salt stress and the less severe reduction in lateral PIN2 shortly after the start of the NaCl treatment in the mutant. In wild-type plants, the subsequent decrease of OSIMS overlaps with an increase in lateral PIN2 levels. In contrast, in *pldζ1* plants persistence of OSIMS coincides with an absence of the in wild-type observed increase in lateral PIN2. This suggests that a processing of OSIMS is required for lateral re-localization of PIN2. However, OSIMS were also found during a 240 mM sorbitol treatment, while the changes in PIN2 distribution between salt- and sorbitol treatment were different (figure 4c-d). This might indicate that the slower processing of the OSIMS and the differences in PIN2 distribution in the *pldζ1*-mutant roots are distinct consequences of the absence of PLDζ1, one that overlaps with a general response to osmotic stress and one that is specific to the ionic component of salt stress. Thus the OSIMS processing might be necessary, but not sufficient for PIN2 lateralisation.

### **A *drp1a* mutant phenocopies the *pldζ1* mutant**

Our data suggest that OSIMS represent excess plasma membrane material, resulting from the loss of turgor due to hyperosmotic shock. To maintain plasma membrane tension, excess membrane material needs to undergo fission and be internalized. The prolonged presence of OSIMS in *pldζ1* root epidermal cells suggests a problem during the fission of this putative excess membrane material. Dynamin-Related Protein 1A (DRP1) has been found to regulate membrane dynamics at the cell plate (Fujimoto et al., 2008) and belongs to the best described fission-related protein family in plants (Collings et al., 2008; Fujimoto et al., 2010; Fujimoto and Tsutsumi, 2014). To test whether DRP1 was involved in the internalization of OSIMS following osmotic stress, PIN2-GFP was imaged in a *drp1a*-mutant background. Like the *pldζ1* mutant, the *drp1a* mutant

contained significantly higher number of OSIMS than wild type after 60 min of salt stress (Figure 7a and b).

### *pldζ1* root epidermal cells have increased cell shrinking during early salt stress response in the elongation zone

If PLD $\zeta$ 1 is involved in membrane trafficking during salt and osmotic stress, then loss of PLD $\zeta$ 1 may lead to defective maintenance of plasma membrane surface area. In guard cells, which shrink and swell through ABA regulation, it has been shown that membrane material is internalized and remobilized back during shrinking and swelling (Shope et al., 2003; Meckel et al., 2004). We investigated root epidermal cell shrinking in the elongation zone of *pldζ1*. Interestingly, an enhanced shrinking of epidermal cells after 5 min of a 120 mM NaCl treatment compared to wild type was found (Figure 8). However, this size reduction disappeared after 60 min in both wild type and *pldζ1* plants (Figure 8). The shorter cells in the *pldζ1* mutant suggest a slower recovery of plasma membrane surface area after cell shrinking due to osmotic stress.

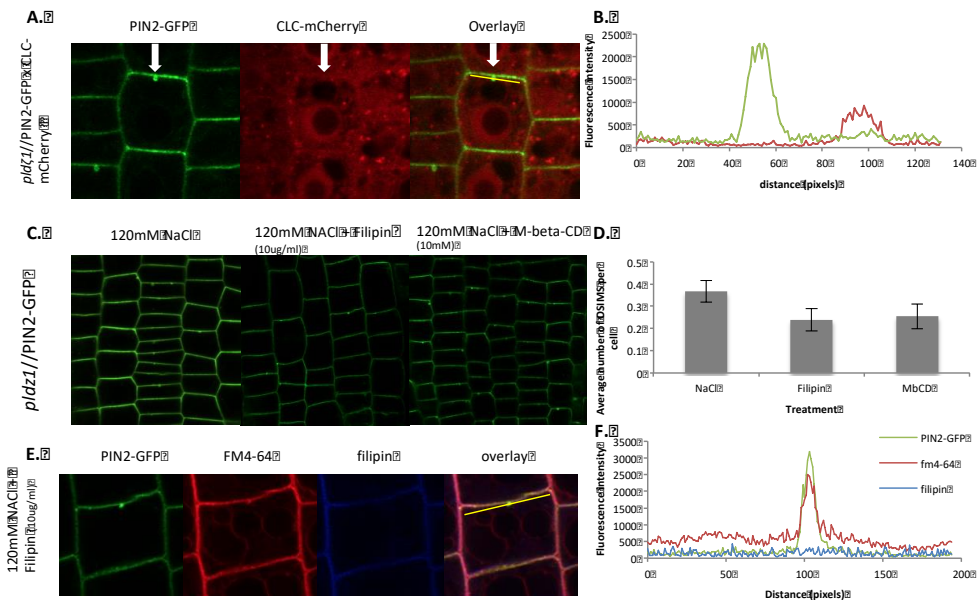


**Figure 6: OSIMS do not co-localize with clathrin light chain and are not inhibited by membrane microdomain inhibiting drugs.** (A) Representative image of a *pldζ1* line expressing PIN2-GFP and CLC2-mCherry during a salt treatment. (B) Profile plot of the yellow line in (A) showing PIN2-GFP and CLC-mCherry intensities just below the apical side of the PM crossing through one OSIMS. (C) Representative images showing a *pldζ1* line expressing PIN2-GFP during salt stress with either no drug, 10ug/ml Filipin or 10mM of Methyl-beta-Cyclodextrin. (D) Quantification of average number of OSIMS per cell during no drug treatment (n=12), Filipin treatment (n=8) and M-b-CD treatment (N=14). No significant differences were found ( $p < 0.05$  in a univariate ANOVA, Tukey post hoc using SPSS 24). (E) Enlargements of one cell expressing PIN2-GFP and stained with fm4-64 and filipin showing one OSIMS. (F) Profile plot the yellow line in (E) showing the OSIMS contains PIN2-GFP and fm4-64 but not filipin.

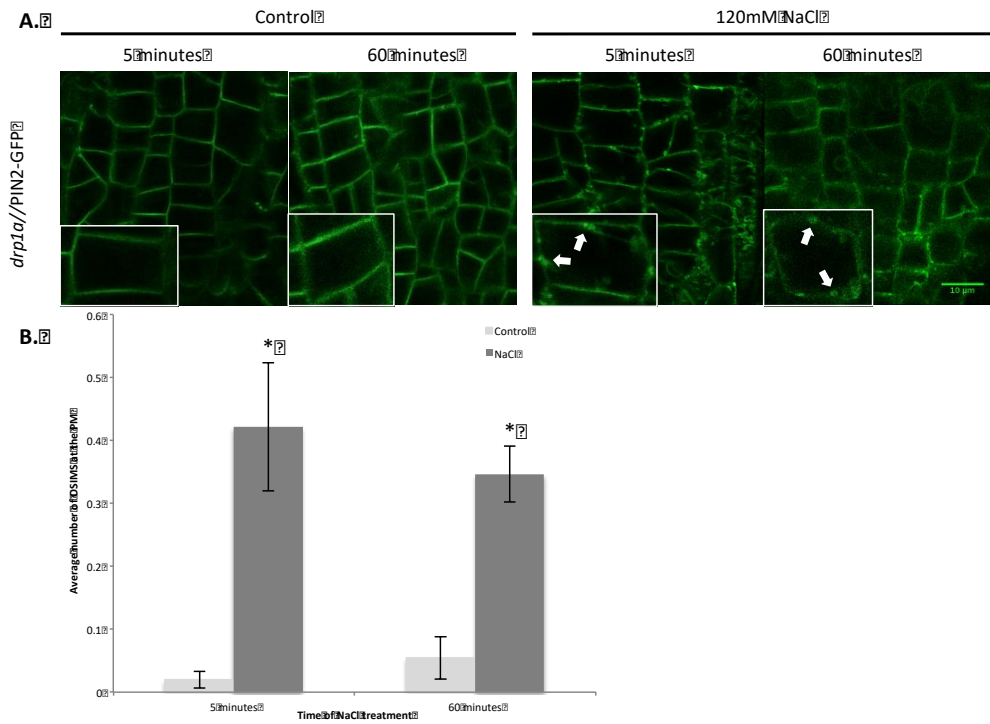


**Figure 7: A *drp1a* mutant has increased OSIMS at the plasma membrane after 60 minutes of salt stress.** (A) Representative pictures of *drp1a* roots expressing PIN2-GFP in control and salt stress conditions. Inlays show one cell enlarged. Arrows point at OSIMS at the plasma membrane. (B) Quantification of the number of OSIMS in the *drp1a* mutant at the plasma membrane per cell in the different treatments. OSIMS were visible after 60 minutes of salt stress. Asterisks show significant differences between the control and salt treatment using a *t*-test ( $p < 0.05$ ) in SPSS 24.

### Loss of PLD $\zeta$ 1 has a mild effect on RSA response to salt

The difference in baseline-PIN2 polarity and salt-induced AUX1 and PIN2 re-localization has been predicted by our model to result in altered auxin dynamics during halotropism in *pld $\zeta$ 1* roots. To determine whether the changes in auxin-transporter dynamics of *pld $\zeta$ 1* roots result in changes in root system architecture (RSA), RSA, we compared root growth parameters of wild-type and *pld $\zeta$ 1* seedlings on agar plates containing 0 or 75 mM NaCl (Figure 9a-f). No differences were found between wildtype and *pld $\zeta$ 1* for main root length (Figure 9a), number of lateral roots (Figure 9b) or lateral root density (Figure 9c) in both control and mild salt stress conditions. However, *pld $\zeta$ 1* plants were found to have on average shorter lateral roots (Figure 9d). Also, *pld $\zeta$ 1* seedlings showed differences in root growth direction for both main- and lateral roots when grown on salt (Figure 9e-f).

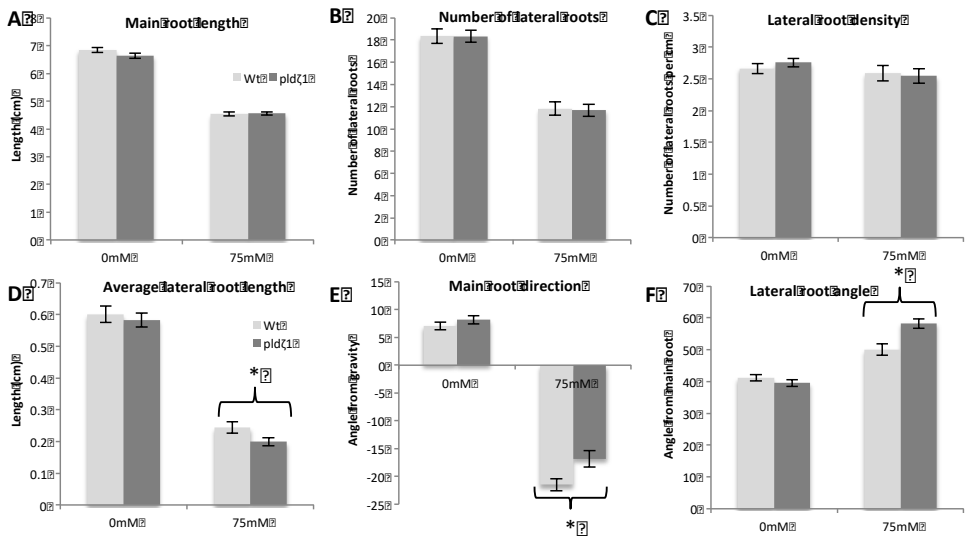
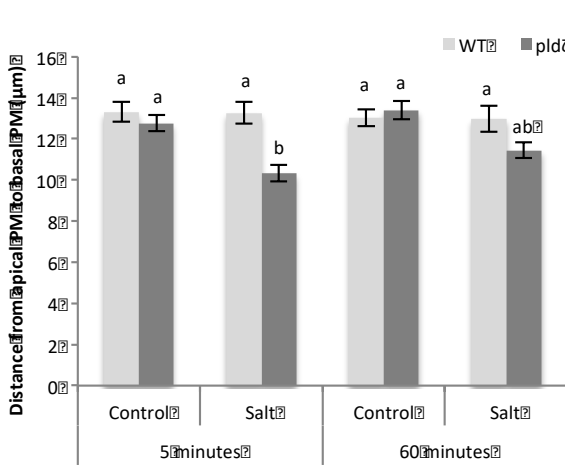


Figure 9: *pldζ1* has shorter lateral roots and both main root and lateral roots grow in a different angle during salt stress. *pldζ1* has no change in main root length (A), number of lateral roots (B) or lateral root density (C). Significant differences that are found are; shorter average lateral root length during mild salt stress (D), main root direction (E), and lateral root direction (F). Results are from 2 biological replicates, total n ± 40. Asterisks show significant differences between Wt and *pldζ1* according to an univariate ANOVA followed by a Tukey post hoc test with p<0.05.

## Discussion

Changes in polar auxin transport in plant roots during development and in response to environmental stimuli are essential for plant survival. So far the endocytosis pathway responsible for internalization of auxin carriers to change polar auxin transport upon stress remains elusive. For the response to salt, both clathrin-dependent and -independent pathways have been proposed (Galvan-Ampudia et al., 2013; Baral et al., 2015). With regards to the clathrin-dependent pathway, PLD $\zeta$ 2 was shown to be involved in PIN2 internalization during salt stress (Galvan-Ampudia et al., 2013). Since the closest homologues of plant PLD $\zeta$ s are mammalian PLDs, which are known to be involved in endocytosis and cell polarity, plant PLD $\zeta$ s are potential candidates for regulating the internalisation of auxin carriers during root responses to tropisms and salt stress. Yet, a role for PLD $\zeta$ 1 in salt-induced auxin carrier internalization had never been addressed.

The results in this study confirm a role for PLD $\zeta$ 1 in tropic responses and salt stress. Furthermore, we observed the formation of large structures at the plasma membrane (OSIMS) shortly after hyperosmotic stress with NaCl or sorbitol. These OSIMS essentially disappeared in wild-type roots within 30 minutes but were still found in *pld $\zeta$ 1* after 60 min hyperosmotic stress. Moreover, re-localization of PIN2 in root epidermal cells upon salt treatment was defective in a *pld $\zeta$ 1* mutant. Furthermore, the lateral AUX1 abundance was found to decrease upon salt stress. Using our previously developed root simulation model (van den Berg et al., 2016), we first demonstrated how salt induced-AUX1 changes could enhance halotropism induced-auxin asymmetry. Additionally, we showed that the observed PIN2-auxin carrier changes in the *pld $\zeta$ 1* mutant lead to a slower build-up of auxin asymmetry during halotropism. Finally, our modeling results showed that it is predominantly the absence of an increase in lateral PIN2 in mutants as compared to wild-type seedlings that reduces auxin asymmetry build-up.

### **PLD $\zeta$ 1 is involved in the halo- and gravitropic response.**

For PLD $\zeta$ 2, a role during halotropism (Galvan-Ampudia et al., 2013), gravitropism (Li and Xue, 2007) and hydrotropism (Taniguchi et al., 2010) has been shown. For PLD $\zeta$ 1, only a role in root hair formation (Ohashi et al., 2003) and root development during phosphate starvation had been described (Li et al., 2006), but not the underlying cellular mechanisms. Here, we report a slower halotropic response of a *pld $\zeta$ 1* mutant. While *pld $\zeta$ 2* had a repressed halotropic

response after 24 hrs of growth on a salt gradient (Galvan-Ampudia et al., 2013), for *pldζ1* a smaller angle away from the salt gradient compared to wildtype after 5-7 hrs was found but no difference after 24 hrs. Additionally, also in contrast to the *pldζ2* mutant (Li and Xue, 2007), which showed a repressed gravitropic response, we found a normal initial- yet a defective attenuation of the long-term gravitropic response for the *pldζ1* mutant. This indicates distinct roles for PLDζ1 and PLDζ2 in the plant root during tropisms. The apparently contrasting result that *pldζ1* mutant had a repressed early-halotropic response and an exaggerated long-term gravitropic response might be explained by the importance of PIN2 re-localization during the early salt response to shift auxin to the non-salt exposed side, and during the late-gravitropic response to attenuate gravitropism. In this way, the dysfunctional PIN2 cycling in *pldζ1* causes the slow start of halotropism and slow ending of gravitropism, underlining the importance of appropriate timing for the distinct roles of PIN2 during tropisms.

### **PLDζ1 regulates PIN2 polarity and auxin carrier polarity shifts during salt stress**

We report altered polarity of PIN2 in a *pldζ1* mutant under control conditions. It is believed that membrane protein polarity is dependent on constitutive cycling, which requires endocytosis and PLDζ2 has been found to be involved in the endocytosis of PIN2 under normal conditions (Li and Xue, 2007). Additionally, it has been shown that PLDζ2 derived PA regulates PIN1 polar localization through an interaction with the scaffolding A1 subunit of Protein Phosphatase 2A (PP2A), which mediates PIN1 dephosphorylation (Gao et al., 2013).

In addition to changes in PIN2 polarization under control conditions in *pldζ1*, PIN2 and AUX1 distribution in *pldζ1* differed from wildtype during respectively later and initial salt stress. This is in agreement with previously shown involvement of PLDζ2 in auxin carrier re-localization during halotropism (Galvan-Ampudia et al., 2013). Moreover, we found similar initial Sorbitol-induced internalization of PIN2 compared to previously reported PIN2 dynamics after a 10 minute mannitol treatment (Zwiewka et al., 2015). So, while salt induces a relocalization of PIN2 to the lateral membrane compartment, osmotic stress does not have this effect. These differences auxin carrier re-localization during salt and osmotic treatments suggest that the re-localization during salt treatment is not due to the osmotic component of the salt stress, and explains why an osmotic gradient does not lead to any tropic response while a salt gradient does (Galvan-Ampudia et al., 2013). Indeed, computational

modelling established that re-localization of PIN2 to the lateral side of the membrane in cells on the salt facing side during halotropism is required for a sufficient difference in auxin concentration between the salt-facing and non-salt facing side of the root (van den Berg et al., 2016).

The involvement of PLD $\zeta$ 2 in PIN endocytosis is proposed to function through the recruitment of components of the clathrin machinery to the PM by binding PLD derived PA (McLoughlin et al., 2013). Interaction between Clathrin-Heavy-Chain (CHC) and Epsin-like Clathrin Adaptor 1 (ECA1) and Epsin-like Clathrin Adaptor 4 (ECA4) and PA was observed shortly after initiation of salt stress. The finding by McLoughlin and colleagues was consistent with other studies showing involvement of clathrin-mediated endocytosis in internalization of auxin carriers (Kleine-Vehn et al., 2010; Galvan-Ampudia et al., 2013; Shinohara et al., 2013; Rakusova et al., 2015; Zwiewka et al., 2015) and aquaporins (Martiniere et al., 2012) during tropic responses or stress by using the CME inhibitor tyrphostinA23 (TyrA23). However, recently it has been shown that TyrA23 treatment results in acidification of the cytoplasm (Dejonghe et al., 2016). This raises serious questions on the specificity of CME inhibition by TyrA23. Other evidence pointing towards clathrin-independent endocytosis during salt stress comes from auxin carriers that are internalized in the presence of NAA, a known inhibitor of CME (Baral et al., 2015). Moreover, ABCB19 is found to interact with PIN1 in association with sterols and sphingolipids (Titapiwatanakun et al., 2009). PIN1 was found in detergent resistant membrane (DRM) fractions after Triton X-100 treatment in wildtype plants while in *abcb19* mutants PIN1 abundance in the DRM fraction was much lower. This suggests that PIN1 internalization through Membrane Microdomain-associated endocytosis (MMAE).

Here, we report unknown structures, approximately 500-700 nm and containing membrane proteins, which arise upon salt and osmotic stress and called them OSIMS. We did not find any evidence hinting towards involvement of clathrin or microdomains with OSIMS. Until today, no strong evidence exists for one specific endocytosis pathway induced during salt stress. However, we report auxin carrier containing excess membrane material, which resides longer at the PM in a *pld $\zeta$ 1* and a *drp1a* mutant, which putatively affects the internalization of auxin carriers during osmotic stress.

### **Loss of PLD $\zeta$ 1 results in a defect in maintaining plasma membrane surface area**

We described novel osmotic stress-induced membrane structures in Arabidopsis seedling roots when treated with NaCl or Sorbitol. Interestingly, these osmotic stress-induced membrane compartments were never observed

detached from the PM. Therefore, we speculate that OSIMS represent excess membrane material due to osmotic stress. Invaginations or folds upon hyperosmotic stress have been observed in yeast (Morris et al., 1983) and it has been proposed that in stomatal guard cell protoplasts, changes in membrane surface area are associated with removal and incorporation of membrane material (Homann, 1998). Likewise, the plasma membrane of isolated rye protoplast (*Secale cereale* L. cv. Puma) cells was found to be smooth after a 50% volume reduction after hyperosmotic stress and internalized vesicles were observed (Gordon-Kamm and Steponkus, 1984). The fact that OSIMS were only observed in the first 30 minutes after NaCl or Sorbitol treatment in wildtype plants and that Arabidopsis epidermal root cells have been shown to recover turgor pressure within 40 minutes after hyperosmotic stress (Shabala and Lew, 2002) supports this theory. To test whether OSIMS are enlarged, growing vesicles we did co-localization experiments with markers for known endocytosis pathways. The OSIMS were not found to co-localize with CLC2 (marker for clathrin coated vesicles) or filipin (a marker for membrane microdomains) suggesting that they are not enlarged vesicles. Consistently, we tested two drugs commonly used to inhibit MMAE to exclude the OSIMS are membrane microdomains that are internalized. First, the sterol depleting agent methyl- $\beta$ -cyclodextrin (M- $\beta$ -CD) has been shown to reduce the abundance of the major structural sterols in the PM by 50% in excised wheat roots (Valitova et al., 2014). We hypothesized that, if OSIMS are membrane microdomains, a 50% structural sterol reduction results in 50% less OSIMS if. However, after application of 10mM M- $\beta$ -CD and 120mM NaCl no reduction in OSIMS was observed. Second, the polyene antibiotic fluorochrome filipin interferes with the function and distribution of sterol in membranes by the induction of cross-linking between sterols. In high concentrations filipin has been successfully used to alter membrane microdomains in yeast (e.g. (Wachtler, 2003)), mammalian cells (e.g. (Shigematsu et al., 2003)) and plant cells (Ovecka et al., 2010). Similar to M- $\beta$ -CD, no differences in OSIMS were observed after filipin treatment. These results support the hypothesis that the OSIMS are excess plasma membrane material induced by hyperosmotic treatment.

The observation that loss of PLD $\zeta$ 1 leads to a slight increase in cell shrinking in root epidermal cells indicates slow recovery of plasma membrane surface area after osmotic stress and thus involvement of PLD $\zeta$ 1 in membrane fission or restoration of osmotic potential.

Evidence in favour of defective OSIMS internalization in the *pld $\zeta$ 1* mutant comes from PA modulating membrane curvature (Kooijman et al., 2003). Likewise, dynamin binding is much more effective in PA-containing

mixed lipid systems (Burger et al., 2000) at the site where fission of the vesicle/compartments needs to take place. Consistently, binding of Drp1 by MitoPLD has been indicated to create a PA-rich microenvironment near the division apparatus of mitochondria (Adachi et al., 2016). Furthermore, the interaction of mammalian PLD2 with dynamin and the involvement of this interaction in endocytosis have been well described (Park et al., 2004; Lee et al., 2006). It has already been proposed that changes in membrane tension due to osmotic stress influence the balance between endo- and exocytosis in order to maintain cell integrity (Zwiewka et al., 2015). Moreover, the involvement of DRP1a in vesicle fission in plants has been reported (Collings et al., 2008; Fujimoto et al., 2010). In these ways PLD $\zeta$ 1 might influence membrane fission during endocytosis or membrane trafficking under osmotic stress. In support, we found a *drp1a* mutant to phenocopy the *pld $\zeta$ 1* mutant regarding OSIMS at the PM after 60 minutes of salt stress, putatively suggesting the involvement of PLD $\zeta$ 1 derived PA in fission of OSIMS. On the other hand, DRP1a mediated endocytosis has been found to affect the polar localization of the borate efflux transporter Requires High Boron 1 (BOR1) (Yoshinari et al., 2016). Furthermore, in the *drp1a* mutant, defective PIN distribution and auxin mediated development is observed (Mravec et al., 2011). This also suggests a role for DRP1a in PIN2 polarity. Summarizing, data provided in this study as well as by others suggests that OSIMS represent osmosis induced excess membrane material, and that PLD $\zeta$ 1 is involved in the subsequent recovery of membrane area and cell shrinking.

### **PLD $\zeta$ 1 is involved in different salt-induced cellular processes**

Our results provide evidence for the involvement of PLD $\zeta$ 1 in baseline PIN2 polarity, auxin carrier re-localization during salt stress, as well as the internalization of salt-induced OSIMS. We propose that PLD $\zeta$ 1 is involved through the effect of PA on plasma membrane characteristics and protein binding of peripheral membrane proteins. For PIN2 polar recycling it was found that changing the phosphorylation at one single site was sufficient to change PIN2 polarity (Zhang et al., 2010). Indeed, protein kinases 3'-phosphoinositide-dependent kinase-1 (PKD1) and PINOID (PID) have been implicated to be involved in PIN polarity (Anthony et al., 2004; Friml et al., 2004; Zegzouti et al., 2006). The PH2 domain of PKD1 is known to have curvature dependent PA binding (Putta et al., 2016). This could explain the effect of PLD $\zeta$ 1 on auxin carrier polarity. As mentioned before PA is also involved in the insertion of DRP1a into the membrane (Burger et al., 2000). So, PA possibly enhances dynamin dependent fission suggesting that PLD $\zeta$ 1 derived PA in the PM might

be involved in the endocytosis of excess membrane material during osmotic stress. Together, this would explain both the differences in PIN2 polarisation as well as the prolonged existence of OSIMS in *pldz1* mutants.

### **Loss of PLD $\zeta$ 1 affects root remodelling during salt stress**

Recently, *pld $\zeta$ 1* growth rate on soil containing 75mM NaCl was found to be more affected than in wildtype while this was not the case for a *pld $\zeta$ 2* mutant (Ben Othman et al., 2017). However, it remains unclear if this is caused by defective root remodelling during salt stress. Different strategies have been described for different Arabidopsis accessions in RSA adaptations to salinity (Julkowska et al., 2014). For the wildtype accession Col-0, it is known that lateral root length (LRL) contribution towards total root size (tRS) increases upon an increase in salt concentration (Julkowska et al., 2014). Thus a shorter main root and longer laterals might be a response to cope with higher salinity. In the current study, we observed in the *pld $\zeta$ 1* mutant a decreased lateral root length to main root length ratio during mild salt stress. Since this represents a reversal of the wildtype salinity response, this supports the idea of defective remodeling in this mutant and suggests a slightly reduced coping capacity of *pld $\zeta$ 1* plants.

### **Lateral AUX1 decrease, PLD $\zeta$ 1 and OSIMS affect the salt response in Arabidopsis roots**

Concluding, we report salt induced changes of AUX1 localization and confirm through mathematical modelling that the observed decrease of lateral AUX1 enhances auxin asymmetry during halotropism. Moreover, this work confirms a role for PLD $\zeta$ 1 in halotropic and gravitropic responses. *pld $\zeta$ 1* mutant were shown to have both permanently altered PIN2 polarity as well as changes in salt induced PIN2 re-localization. Simulations in our updated root model show how these differences result in delayed and weaker build-up of auxin asymmetry in the *pld $\zeta$ 1* mutant thus explaining its halotropism phenotype. Finally, we discovered novel osmotic stress induced membrane structures (OSIMS). The hampered processing of OSIMS in the *pld $\zeta$ 1* mutant coincides with the absence of PIN2 re-localization to the lateral side of the PM during salt stress and thus indicates a role for OSIMS in the auxin carrier dynamics during salt stress. Together, these results further our knowledge on auxin carrier internalization and re-localization during the salt stress response.

## Methods

### Plant materials and growth conditions

The wild type used was *Arabidopsis thaliana*, ecotype Columbia-0 (Col-0). The *pldζ1* mutant is a T-DNA insertion line (SALK\_083090). The PIN2-GFP/*pldζ1*, AUX1-mVenus/*pldζ1*, RabF2b-RFPxPIN2-GFP, SYP32-RFPxPIN2-GFP, RabA1e-RFPxPIN2-GFP, VHA1-RFPxPIN2-GFP, RabF2b-RFPxPIN2-GFP/*pldζ1*, SYP32-RFPxPIN2-GFP/*pldζ1*, RabA1e-RFPxPIN2-GFP/*pldζ1*, VHA1-RFPxPIN2-GFP/*pldζ1*, PLDζ 1-YFP/*pldζ1* were created by crossing the following published lines: PIN2-GFP (Xu and Scheres, 2005), AUX1-mVenus (Band et al., 2014), *drp1a*/PIN2-GFP (Mravec et al., 2011) RabF2b-RFP, SYP32-RFP, RabA1e-RFP (Geldner et al., 2009) and VHA1-RFP (Dettmer et al., 2006). Primers used for *pldζ1* genotyping are: forward, tgaaaagcatggaattttcg and reverse, gtgatcgtctctgtctctcgc. General growth conditions on agar plates (half strength MS supplemented with 0.1% 2(N-morpholino)ethanesulphonic acid (MES) buffer and 0.5% Sucrose and 1% Agar) were in a climate chamber with long day period (16 hrs light at 130 μmol/m<sup>2</sup>/s) at 22°C and 70% humidity. Seeds were sterilized using 50% bleach and stratified for at least 2 days at 4°C. For soil experiments, seeds sterilized with 50% bleach were stratified in 0.1% agar in the dark for at least 2 days and then placed on sieved sowing ground. Plants were then grown were in a climate chamber with short day period (11 hrs light at 130 μmol/m<sup>2</sup>/s) at 22°C and 70% humidity.

### Halotropism plate assays and gravitropism plate assays

For the halotropism plate assays (both during timelapse imaging and long-term halotropism assays) 10 seeds were germinated in a diagonal line on half strength MS plates. When the seedlings were 5 days old, the bottom corner (in diagonal line 0,5 cm below the root tips) of the agar was removed and replaced by control half strength MS agar without salt or half strength MS agar containing 200mM NaCl. For the time-lapse experiment the plates were placed in a climate chamber containing the time-lapse set-up. Here, all plates were imaged every 20 minutes by infrared photography. Images were then analysed using Imaj. For the long-term halotropism assay a dot was placed immediately after replacing the agar and every 24 hours after the start of the treatment. After 4 days of growth the plates were scanned and the images were analysed using ImageJ. In the gravitropism assay 12 plants were germinated on half strength MS plates and after 5 days of growth the plates were re-orientated by turning 90 degrees and placed in the climate chamber containing the time-lapse set-up. All plates were imaged every 20 minutes by infrared photography. Images were analysed using Imaj.

### Confocal microscopy

The images were acquired using a Nikon Ti inverted microscope in combination with an A1 spectral confocal scanning head. For all GFP fusion proteins excitation/emission wavelengths used were 488 nm/505-555 nm. For mVenus excitation/emission wavelengths were 514 nm/525-555 nm. For mCherry and RFP excitation/emission wavelengths were 561 nm/570-620 nm. The analysis of the images was performed

using Fiji (<http://fiji.sc>) software. Using a confocal microscope with a 60x objective did not yield a resolution high enough to distinguish between the apical membrane of one cell with the basal membrane of the neighbouring cell. For AUX1-mVenus we measured both and added them up to create the apical/basal component. All images were corrected for background signal.

Membrane intensity quantification was done using ImageJ, for all cells the average pixel intensity for the apical side (or apical/basal in the case of AUX1 and PMA2), and both lateral sides of the PM and the intracellular signal was measured by drawing a region of interest (ROI) by hand.

OSIMS quantification was done using ImageJ, a structure was classified as an OSIM structure when it was attached to the PM but clearly on the cytosolic side of the PM and larger than 300 nm. Drug treatments were performed as follows: for filipin, seedlings were treated/stained with 10 µg/ml filipin for one hour after which 120mM NaCl was added and plants were stressed for 60 minutes. For Methyl-beta-Cyclodextrin, seedlings were treated with 10 mM M-β-CD for one hour after which 120mM NaCl was added and plants were stressed for 60 minutes.

### **Model adjustments**

Our current study makes use of a previously developed model described in detail in (van den Berg et al., 2016). Briefly, the model consists of a detailed two-dimensional cross section of the Arabidopsis root tip, incorporating cell-type and developmental zone specific differences in cell sizes, and patterns of the auxin-exporting PIN and auxin importing AUX/LAX proteins. Auxin dynamics, production, degradation, intracellular and apoplast diffusion and across membrane fluxes- are computed on a subcellular grid level resolution, while gene expression is simulated at the level of individual cells. In addition, we include that for AUX/LAX gene expression is auxin dependent while for PIN2 membrane occupancy levels are auxin dependent.

Relative to this earlier study a few minor changes were implemented. First, to increase computational precision, simulations were performed with a spatial integration step of 1 rather than 2microm, resulting in a factor 4 increase in the number of simulated grid points together constituting the root tissue. Second, to increase physiological realism, a more gradual increase in the size of cells in the early elongation zone was incorporated. For further details we refer to our earlier study.

### **Main modeling assumptions**

To apply the experimentally obtained data to our (halo)tropism model, we needed to make two key assumptions. First, salt induced effects on intracellular and membrane protein patterns were measured under experimental conditions in which salt was uniformly applied to the plant roots. To extrapolate these findings to halotropism where salt stress occurs (predominantly) at a single side of the root, we assumed that the experimentally observed changes in PIN2 and AUX1 occur in a similar manner but only at the salt exposed side of the root.

Second, in contrast to our earlier work microscopic images were obtained using a longitudinal epidermal top view rather than a longitudinal cross section of the root. As a consequence, in addition to apical and basal membranes, radial rather than transversal lateral membrane faces were imaged. To extrapolate the thus obtained data to our halotropism model, which describes a longitudinal cross section, we assumed that PIN2 and AUX1 patterns on radial and transversal lateral membranes are similar. Support for this assumption can be derived from the observation that similar to what we previously observed for wildtype PIN2 on transversal lateral membranes (Galvan-Ampudia et al., 2013) wildtype PIN2 on radial lateral membranes was observed to decrease approximately 20% in response to salt exposure.

### **Simulating *pldζ1* mutants**

Our experimental data indicate that *pldζ1* mutants have an approximately 15% reduction in apical PIN2 levels and an approximately 10% increase in (inward) lateral PIN2 levels under control conditions. As we model standard wildtype epidermal cells under control conditions to have a ratio of PIN2 apical: lateral of 1:0.1, we thus simulate *pldζ1* epidermal cells under control conditions as having a ratio of apical PIN2: lateral PIN2 of 0.85:0.11 (Supplemental figure S3). Notably, this results in a less polar PIN2 pattern, as well as a lower overall PIN2 level. These differences in PIN2 pattern result in minor changes in the default, non-halotropic auxin pattern of *pldζ1* as compared to wildtype roots (Supplemental figure S3).

Our experimental data indicate that in addition to changes in PIN2, cellular AUX1 patterns also change in response to salt exposure, with apical/basal levels recovering after a transient change and lateral levels showing a longer term, approximately 20% decrease. Therefore, in most halotropism simulations (indicated), we incorporated a 20% reduction of AUX1 on the lateral membranes of epidermal cells on the salt exposed side of the root.

### **Root system architecture assay**

*pldζ1* and WT plants were germinated on half strength MS plates. Four days after germination the seedlings were transferred to half strength MS plates with either 0mM, 75mM and 125 mM of NaCl. Four seedlings were transferred to each plate, resulting in 20 replicas per line per treatment. Plates were placed in the climate chamber following a randomized order. After 6 days the plates were scanned using an Epson Perfection V800 scanner at a resolution of 400 dpi. Root phenotypes were quantified using the SmartRoot (Lobet et al., 2011) plugin for ImageJ. Statistical analysis was performed in R with RStudio using two-way ANOVA with Tukey's post hoc test for significance.

### **Acknowledgements**

We thank Remko Offringa (PIN2-GFP), Malcolm Bennet (AUX1-mVenus), Jiri Friml (PIN2-GFP/*drp1a*), Niko Geldner (wavelines W2R, W22R and W34R)(Geldner et al., 2009), Karin Schumacher (VHA1-RFP and PMA2-GFP)

and Eva Benkova (PIN3-GFP) for kindly sharing published materials. We thank Michel Haring and Teun Munnik for critical reading. This project was funded by NWO (CW 711.014.002).

## References

- Adachi Y, Itoh K, Yamada T, Cerveny KL, Suzuki TL, Macdonald P, Frohman MA, Ramachandran R, Iijima M, Sesaki H** (2016) Coincident Phosphatidic Acid Interaction Restrains Drp1 in Mitochondrial Division. *Mol Cell* **63**: 1034-1043
- Adamowski M, Friml J** (2015) PIN-dependent auxin transport: action, regulation, and evolution. *Plant Cell* **27**: 20-32
- Anthony RG, Henriques R, Helfer A, Meszaros T, Rios G, Testerink C, Munnik T, Deak M, Koncz C, Bogre L** (2004) A protein kinase target of a PDK1 signalling pathway is involved in root hair growth in Arabidopsis. *the EMBO Journal* **23**: 572-581
- Armengot L, Marques-Bueno MM, Jaillais Y** (2016) Regulation of polar auxin transport by protein and lipid kinases. *J Exp Bot* **67**: 4015-4037
- Band LR, Wells DM, Fozard JA, Ghetiu T, French AP, Pound MP, Wilson MH, Yu L, Li W, Hijazi HI, Oh J, Pearce SP, Perez-Amador MA, Yun J, Kramer E, Alonso JM, Godin C, Vernoux T, Hodgman TC, Pridmore TP, Swarup R, King JR, Bennett MJ** (2014) Systems analysis of auxin transport in the Arabidopsis root apex. *Plant Cell* **26**: 862-875
- Baral A, Irani NG, Fujimoto M, Nakano A, Mayor S, Mathew MK** (2015) Salt-Induced Remodeling of Spatially Restricted Clathrin-Independent Endocytic Pathways in Arabidopsis Root. *Plant Cell*: tpc-15
- Bargmann BO, Laxalt AM, ter Riet B, van Schooten B, Merquiol E, Testerink C, Haring MA, Bartels D, Munnik T** (2009) Multiple PLDs required for high salinity and water deficit tolerance in plants. *Plant Cell Physiol* **50**: 78-89
- Ben Othman A, Ellouzi H, Planchais S, De Vos D, Faiyue B, Carol P, Abdelly C, Savoure A** (2017) Phospholipases Dzeta1 and Dzeta2 have distinct roles in growth and antioxidant systems in Arabidopsis thaliana responding to salt stress. *Planta* **246**: 721-735
- Berendsen RL, Pieterse CM, Bakker PA** (2012) The rhizosphere microbiome and plant health. *Trends Plant Sci* **17**: 478-486
- Burger KNJ, Demel RA, Schmid SL, Kruijff de B** (2000) Dynamin Is Membrane-Active: Lipid Insertion Is Induced by Phosphoinositides and Phosphatidic Acid. *Biochemistry* **2000**: 12485-12493
- Collings DA, Gebbie LK, Howles PA, Hurley UA, Birch RJ, Cork AH, Hocart CH, Arioli T, Williamson RE** (2008) Arabidopsis dynamin-like protein DRP1A: a null mutant with widespread defects in endocytosis, cellulose synthesis, cytokinesis, and cell expansion. *J Exp Bot* **59**: 361-376
- Dejonghe W, Kuenen S, Mylle E, Vasileva M, Keech O, Viotti C, Swerts J, Fendrych M, Ortiz-Morea FA, Mishev K, Delang S, Scholl S, Zarza X, Heilmann M, Kourelis J, Kasproicz J, Nguyen le SL, Drozdzecki A, Van Houtte I, Szatmari AM, Majda M, Baisa G, Bednarek SY, Robert S, Audenaert D, Testerink C, Munnik T, Van Damme D, Heilmann I, Schumacher K, Winne J, Friml J, Verstreken P, Russinova E** (2016) Mitochondrial uncouplers

inhibit clathrin-mediated endocytosis largely through cytoplasmic acidification. *Nat Commun* **7**: 11710

- Dettmer J, Hong-Hermesdorf A, Stierhof YD, Schumacher K** (2006) Vacuolar H<sup>+</sup>-ATPase activity is required for endocytic and secretory trafficking in Arabidopsis. *Plant Cell* **18**: 715-730
- Di Mambro R, De Ruvo M, Pacifici E, Salvi E, Sozzani R, Benfey PN, Busch W, Novak O, Ljung K, Di Paola L, Maree AFM, Costantino P, Grieneisen VA, Sabatini S** (2017) Auxin minimum triggers the developmental switch from cell division to cell differentiation in the Arabidopsis root. *Proc Natl Acad Sci U S A* **114**: E7641-E7649
- Donaldson JG** (2009) Phospholipase D in endocytosis and endosomal recycling pathways. *Biochim Biophys Acta* **1791**: 845-849
- Du G, Huang P, Liang BT, Frohman MA** (2004) Phospholipase D2 Localizes to the Plasma Membrane and Regulates Angiotensin II Receptor Endocytosis. *Mol Biol Cell* **15**: 1024-1030
- Frank W, Munnik T, Kerkmann K, Salamani F, Bartels D** (2000) Water Deficit Triggers Phospholipase D Activity in the Resurrection Plant *Craterostigma plantagineum*. *Plant Cell* **12**: 111-123
- Friml J, Yang X, Michniewicz M, Weijers D, Quint A, Tietz O, Benjamins R, Ouwerkerk PB, Ljung K, Sandberg G, Hooykaas PJ, Palme K, Offringa R** (2004) A PINOID-dependent binary switch in apical-basal PIN polar targeting directs auxin efflux. *Science* **306**: 862-865
- Fujimoto M, Arimura S, Nakazono M, Tsutsumi N** (2008) Arabidopsis dynamin-related protein DRP2B is co-localized with DRP1A on the leading edge of the forming cell plate. *Plant Cell Rep* **27**: 1581-1586
- Fujimoto M, Arimura S, Ueda T, Takanashi H, Hayashi Y, Nakano A, Tsutsumi N** (2010) Arabidopsis dynamin-related proteins DRP2B and DRP1A participate together in clathrin-coated vesicle formation during endocytosis. *Proc Natl Acad Sci U S A* **107**: 6094-6099
- Fujimoto M, Tsutsumi N** (2014) Dynamin-related proteins in plant post-Golgi traffic. *Front Plant Sci* **5**: 408
- Galvan-Ampudia CS, Julkowska MM, Darwish E, Gandullo J, Korver RA, Brunoud G, Haring MA, Munnik T, Vernoux T, Testerink C** (2013) Halotropism is a response of plant roots to avoid a saline environment. *Curr Biol* **23**: 2044-2050
- Gao HB, Chu YJ, Xue HW** (2013) Phosphatidic acid (PA) binds PP2AA1 to regulate PP2A activity and PIN1 polar localization. *Mol Plant* **6**: 1692-1702
- Geldner N, Denervaud-Tendon V, Hyman DL, Mayer U, Stierhof YD, Chory J** (2009) Rapid, combinatorial analysis of membrane compartments in intact plants with a multicolor marker set. *The Plant Journal* **59**: 169-178
- Geng Y, Wu R, Wee CW, Xie F, Wei X, Chan PM, Tham C, Duan L, Dinneny JR** (2013) A spatio-temporal understanding of growth regulation during the salt stress response in Arabidopsis. *Plant Cell* **25**: 2132-2154
- Gordon-Kamm WJ, Steponkus PI** (1984) The Behavior of the Plasma Membrane Following Osmotic Contraction of Isolated Protoplasts: Implications in Freezing Injury. *Protoplasma* **123**: 83-94
- Heuser J** (1980) Three-dimensional visualization of coated vesicle formation in fibroblasts. *J Cell Biol* **84**: 560-583

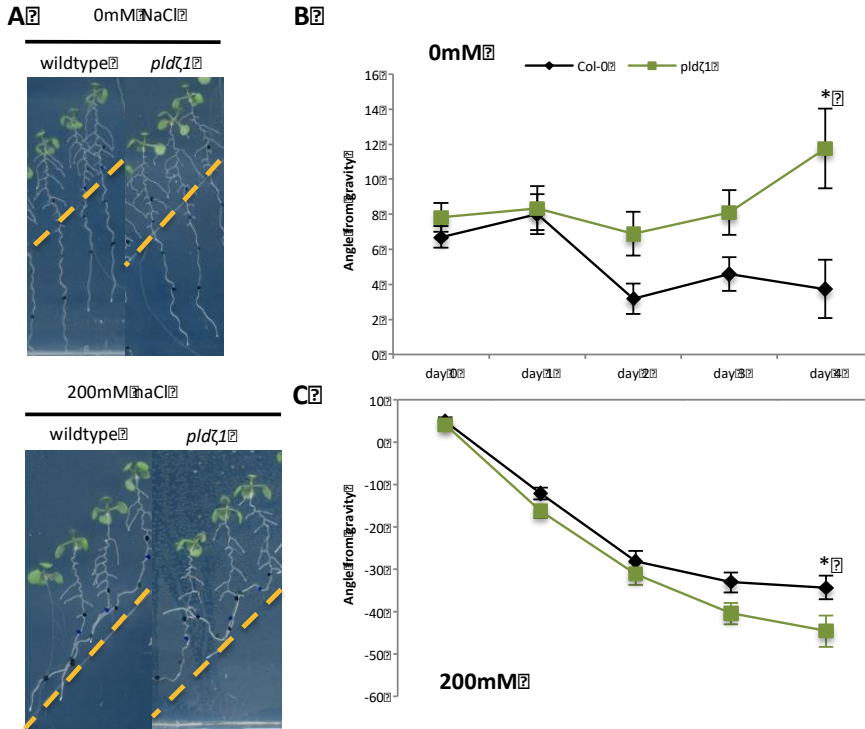
- Homann U** (1998) Fusion and Fission of plasma-membrane material accommodates for osmotically induced changes in the surface area of guard-cell protoplasts. *Planta* **206**: 329-333
- Jacob T, Ritchie S, Assmann SM, Gilroy S** (1999) Abscisic acid signal transduction in guard cells is mediated by phospholipase D activity. *Proc Natl Acad Sci U S A* **96**: 12192-12197
- Jiang Y, Sverdlov MS, Toth PT, Huang LS, Du G, Liu Y, Natarajan V, Minshall RD** (2016) Phosphatidic Acid Produced by RalA-activated PLD2 Stimulates Caveolae-mediated Endocytosis and Trafficking in Endothelial Cells. *J Biol Chem* **291**: 20729-20738
- Julkowska MM, Hoefsloot HC, Mol S, Feron R, de Boer GJ, Haring MA, Testerink C** (2014) Capturing Arabidopsis root architecture dynamics with ROOT-FIT reveals diversity in responses to salinity. *Plant Physiol* **166**: 1387-1402
- Julkowska MM, Koevoets IT, Mol S, Hoefsloot H, Feron R, Testerink MA, Keurentjes JJB, Korte A, Haring MA, de Boer GJ, Testerink C** (2017) Genetic Components of Root Architecture Remodeling in Response to Salt Stress. *Plant Cell* **29**: 3198-3213
- Julkowska MM, Testerink C** (2015) Tuning plant signaling and growth to survive salt. *Trends Plant Sci* **20**: 586-594
- Kleine-Vehn J, Ding Z, Jones AR, Tasaka M, Morita MT, Friml J** (2010) Gravity-induced PIN transcytosis for polarization of auxin fluxes in gravity-sensing root cells. *Proc Natl Acad Sci U S A* **107**: 22344-22349
- Kochian LV, Pinerros MA, Liu J, Magalhaes JV** (2015) Plant Adaptation to Acid Soils: The Molecular Basis for Crop Aluminum Resistance. *Annu Rev Plant Biol* **66**: 571-598
- Kooijman EE, Chupin V, Kruijff de B, Burger KNJ** (2003) Modulation of Membrane Curvature by Phosphatidic Acid and Lysophosphatidic acid. *Traffic* **4**: 162-174
- Laskowski M, Grieneisen VA, Hofhuis H, Hove CA, Hogeweg P, Maree AF, Scheres B** (2008) Root system architecture from coupling cell shape to auxin transport. *PLoS Biol* **6**: e307
- Lee CS, Kim IS, Park JB, Lee MN, Lee HY, Suh PG, Ryu SH** (2006) The phox homology domain of phospholipase D activates dynamin GTPase activity and accelerates EGFR endocytosis. *Nat Cell Biol* **8**: 477-484
- Li G, Xue HW** (2007) Arabidopsis PLDzeta2 regulates vesicle trafficking and is required for auxin response. *Plant Cell* **19**: 281-295
- Li M, Qin C, Welti R, Wang X** (2006) Double knockouts of phospholipases Dzeta1 and Dzeta2 in Arabidopsis affect root elongation during phosphate-limited growth but do not affect root hair patterning. *Plant Physiol* **140**: 761-770
- Lobet G, Pages L, Draye X** (2011) A novel image-analysis toolbox enabling quantitative analysis of root system architecture. *Plant Physiol* **157**: 29-39
- Martiniere A, Li X, Runions J, Lin J, Maurel C, Luu DT** (2012) Salt stress triggers enhanced cycling of Arabidopsis root plasma-membrane aquaporins. *Plant Signal Behav* **7**: 529-532
- McDermott M, Wakelam MJ, Morris AJ** (2004) Phospholipase D. *Biochem Cell Biol* **82**: 225-253
- McLoughlin F, Arisz SA, Dekker HL, Kramer G, de Koster CG, Haring MA, Munnik T, Testerink C** (2013) Identification of novel candidate phosphatidic acid-binding proteins involved in the salt-stress response of Arabidopsis thaliana roots. *Biochem J* **450**: 573-581

- Meckel T, Hurst AC, Thiel G, Homann U** (2004) Endocytosis against high turgor: intact guard cells of *Vicia faba* constitutively endocytose fluorescently labelled plasma membrane and GFP-tagged K-channel KAT1. *Plant J* **39**: 182-193
- Morris GJ, Winters L, Coulson GE, Clarke KJ** (1983) Effect of Osmotic Stress on the Ultrastructure and Viability of the Yeast *Saccharomyces cerevisiae*. *Microbiology* **132**: 2023-2034
- Mravec J, Petrasek J, Li N, Boeren S, Karlova R, Kitakura S, Parezova M, Naramoto S, Nodzynski T, Dhonukshe P, Bednarek SY, Zazimalova E, de Vries S, Friml J** (2011) Cell plate restricted association of DRP1A and PIN proteins is required for cell polarity establishment in Arabidopsis. *Curr Biol* **21**: 1055-1060
- Munnik T** (2001) Phosphatidic acid: an emerging plant lipid second messenger. *Trends Plant Sci* **6**: 227-233
- Munnik T, Meijer HJG, ter Riet B, Hirt H, Wolfgang F, Bartels D, Musgrave A** (2000) Hyperosmotic stress stimulates phospholipase D activity and elevates the levels of phosphatidic acid and diacylglycerol pyrophosphate. *Plant J* **22**: 147-154
- Munns R, Gilliham M** (2015) Salinity tolerance of crops - what is the cost? *New Phytol* **208**: 668-673
- Naramoto S** (2017) Polar transport in plants mediated by membrane transporters: focus on mechanisms of polar auxin transport. *Curr Opin Plant Biol* **40**: 8-14
- Ohashi Y, Oka A, Rodrigues-Pousada R, Possenti M, Ruberti I, Morelli G, Aoyama T** (2003) Modulation of Phospholipid Signaling by GLABRA2 in Root-Hair Pattern Formation. *Science* **300**: 1427-1430
- Ovecka M, Berson T, Beck M, Derksen J, Samaj J, Baluska F, Lichtscheidl IK** (2010) Structural sterols are involved in both the initiation and tip growth of root hairs in *Arabidopsis thaliana*. *Plant Cell* **22**: 2999-3019
- Park JB, Lee CS, Lee HY, Kim IS, Lee BD, Jang IH, Jung YW, Oh YS, Han MY, Jensen ON, Roepstorff P, Suh PG, Ryu SH** (2004) Regulation of phospholipase D2 by GTP-dependent interaction with dynamin. *Adv Enzyme Regul* **44**: 249-264
- Pleskot R, Pejchar P, Bezdova R, Lichtscheidl IK, Wolters-Arts M, Marc J, Zarsky V, Potocky M** (2012) Turnover of Phosphatidic Acid through Distinct Signaling Pathways Affects Multiple Aspects of Pollen Tube Growth in Tobacco. *Front Plant Sci* **3**: 54
- Putta P, Rankenberg J, Korver RA, van Wijk R, Munnik T, Testerink C, Kooijman EE** (2016) Phosphatidic acid binding proteins display differential binding as a function of membrane curvature stress and chemical properties. *Biochim Biophys Acta* **1858**: 2709-2716
- Qin C, Wang X** (2002) The Arabidopsis Phospholipase D Family. Characterization of a Calcium-Independent and Phosphatidylcholine-Selective PLDzeta 1 with Distinct Regulatory Domains. *Plant Physiology* **128**: 1057-1068
- Rakusova H, Fendrych M, Friml J** (2015) Intracellular trafficking and PIN-mediated cell polarity during tropic responses in plants. *Curr Opin Plant Biol* **23**: 116-123
- Shabala SN, Lew RR** (2002) Turgor regulation in osmotically stressed Arabidopsis epidermal root cells. Direct support for the role of inorganic ion uptake as revealed by concurrent flux and cell turgor measurements. *Plant Physiol* **129**: 290-299

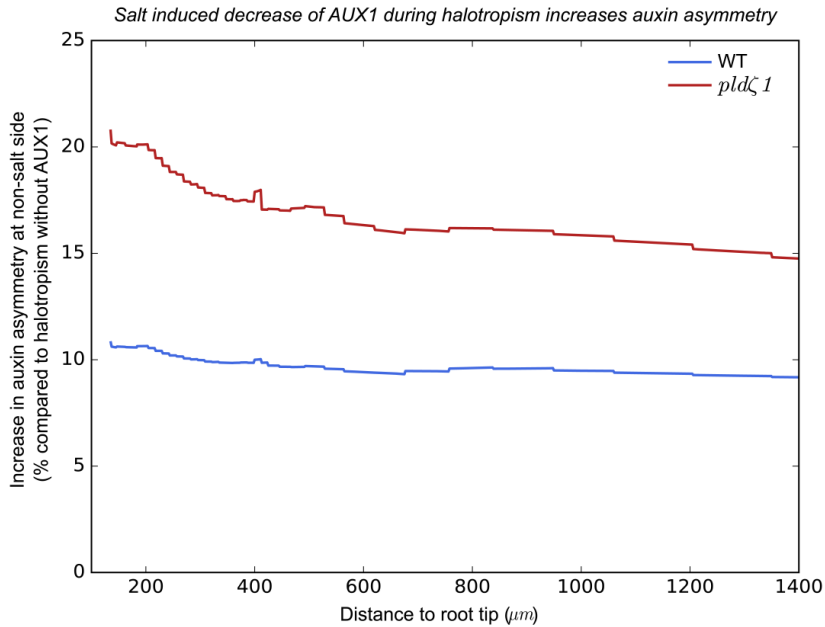
- Shigematsu S, Watson RT, Khan AH, Pessin JE** (2003) The adipocyte plasma membrane caveolin functional/structural organization is necessary for the efficient endocytosis of GLUT4. *J Biol Chem* **278**: 10683-10690
- Shinohara N, Taylor C, Leyser O** (2013) Strigolactone can promote or inhibit shoot branching by triggering rapid depletion of the auxin efflux protein PIN1 from the plasma membrane. *PLoS Biol* **11**: e1001474
- Shope JC, DeWald DB, Mott KA** (2003) Changes in surface area of intact guard cells are correlated with membrane internalization. *Plant Physiol* **133**: 1314-1321
- Su W, Yeku O, Olepu S, Genna A, Park JS, Ren H, Du G, Gelb MH, Morris AJ, Frohman MA** (2009) 5-Fluoro-2-indolyl des-chlorohalopemide (FIPI), a phospholipase D pharmacological inhibitor that alters cell spreading and inhibits chemotaxis. *Mol Pharmacol* **75**: 437-446
- Takac T, Pechan T, Samajova O, Ovecka M, Richter H, Eck C, Niehaus K, Samaj J** (2012) Wortmannin treatment induces changes in Arabidopsis root proteome and post-Golgi compartments. *J Proteome Res* **11**: 3127-3142
- Taniguchi YY, Taniguchi M, Tsuge T, Oka A, Aoyama T** (2010) Involvement of Arabidopsis thaliana phospholipase D $\zeta$ 2 in root hydrotropism through the suppression of root gravitropism. *Planta* **231**: 491-497
- Testerink C, Munnik T** (2011) Molecular, cellular, and physiological responses to phosphatidic acid formation in plants. *J Exp Bot* **62**: 2349-2361
- Titapiwatanakun B, Blakeslee JJ, Bandyopadhyay A, Yang H, Mravec J, Sauer M, Cheng Y, Adamec J, Nagashima A, Geisler M, Sakai T, Friml J, Peer WA, Murphy AS** (2009) ABCB19/PGP19 stabilises PIN1 in membrane microdomains in Arabidopsis. *Plant J* **57**: 27-44
- Valitova J, Sulkarnayeva A, Kotlova E, Ponomareva A, Mukhitova FK, Murtazina L, Ryzhkina I, Beckett R, Minibayeva F** (2014) Sterol binding by methyl-beta-cyclodextrin and nystatin--comparative analysis of biochemical and physiological consequences for plants. *FEBS J* **281**: 2051-2060
- van den Berg T, Korver RA, Testerink C, Ten Tusscher KH** (2016) Modeling halotropism: a key role for root tip architecture and reflux loop remodeling in redistributing auxin. *Development* **143**: 3350-3362
- Wachtler V** (2003) Sterol-rich plasma membrane domains in the fission yeast *Schizosaccharomyces pombe*. *J Cell Sci* **116**: 867-874
- Wicke B, Smeets E, Dornburg V, Vashev B, Gaiser T, Turkenburg W, Faaij A** (2011) The global technical and economic potential of bioenergy from salt-affected soils. *Energy & Environmental Science* **4**: 2669
- Xu J, Scheres B** (2005) Dissection of Arabidopsis ADP-RIBOSYLATION FACTOR 1 function in epidermal cell polarity. *Plant Cell* **17**: 525-536
- Yao HY, Xue HW** (2018) Phosphatidic acid plays key roles regulating plant development and stress responses. *J Integr Plant Biol*
- Yoshinari A, Fujimoto M, Ueda T, Inada N, Naito S, Takano J** (2016) DRP1-Dependent Endocytosis is Essential for Polar Localization and Boron-Induced Degradation of the Borate Transporter BOR1 in Arabidopsis thaliana. *Plant Cell Physiol* **57**: 1985-2000
- Zegzouti H, Anthony RG, Jahchan N, Bogre L, Christensen SK** (2006) Phosphorylation and activation of PINOID by the phospholipid signaling kinase 3-phosphoinositide-dependent protein kinase 1 (PKD1) in Arabidopsis. *Proc Natl Acad Sci U S A* **103**: 6404-6409

- Zhang J, Nodzynski T, Pencik A, Rolcik J, Friml J** (2010) PIN phosphorylation is sufficient to mediate PIN polarity and direct auxin transport. *Proc Natl Acad Sci U S A* **107**: 918-922
- Zwiewka M, Nodzynski T, Robert S, Vanneste S, Friml J** (2015) Osmotic Stress Modulates the Balance between Exocytosis and Clathrin-Mediated Endocytosis in *Arabidopsis thaliana*. *Mol Plant* **8**: 1175-1187

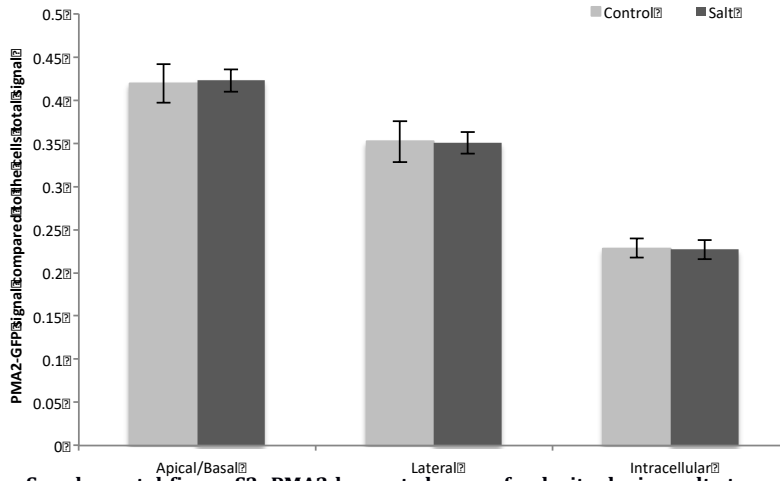
## Supplemental information



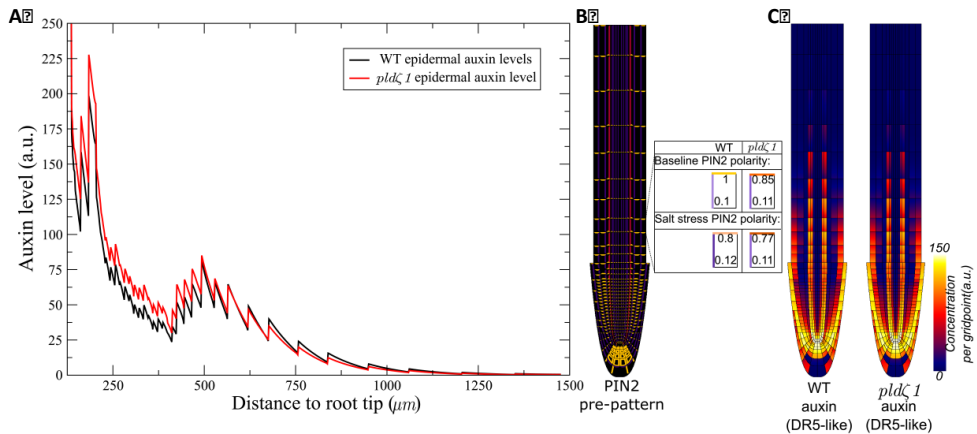
**Supplemental figure S1: Long term effects on halotropic response show delayed attenuation of the halotropic response.** (A) Images showing 5 days of growth of WT and the *pldζ1* mutant on gradient plates with 0mM or 200mM of NaCl. (B,C) Quantification of halotropism plate assay over multiple days shows more skewing of *pldζ1* mutant roots in control conditions (B) (3 biological replicates: WT n=68, *pldζ1* n=62) and more avoidance after 4 days of growth on a salt medium (C) (3 biological replicates: WT n=67, *pldζ1* n=66). Asterisks show significant differences, an univariate ANOVA was used followed by a Tukey post-hoc test ( $p < 0.05$ )



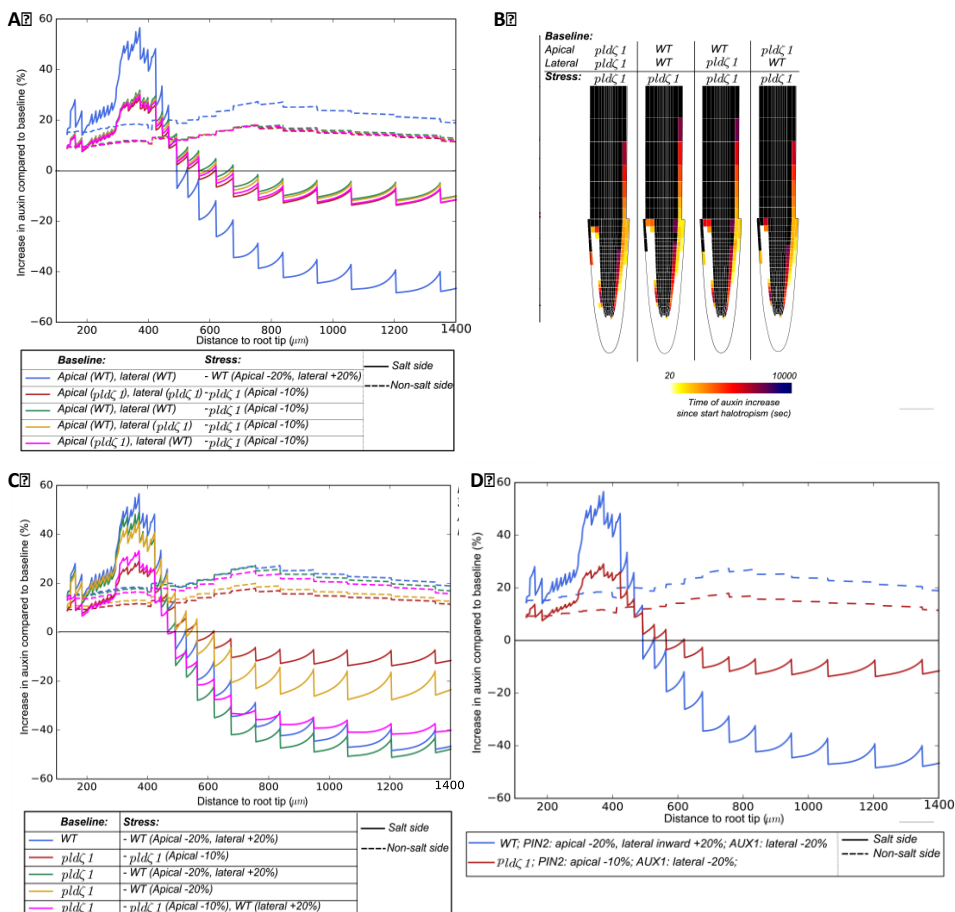
**Supplemental figure S2: Quantification of the effect of salt induced changes in AUX1 patterning on auxin asymmetry.** Percentage increase in the auxin elevation occurring at the non-salt exposed side of the root as a consequence of incorporating salt induced changes in AUX1 patterning for both wildtype and *pld $\zeta$ 1* plants.



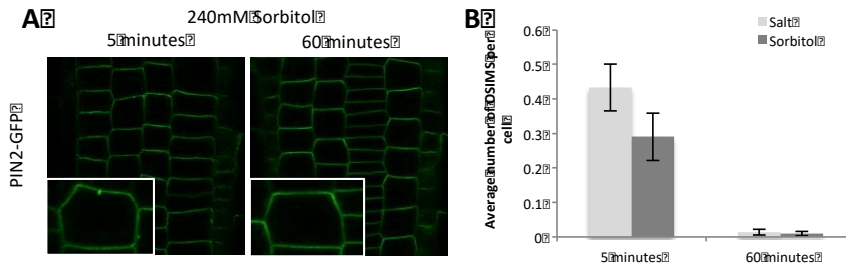
**Supplemental figure S3: PMA2 has not change of polarity during salt stress.** PMA2-GFP expressing seedlings were treated with either control or salt containing (120mM NaCl) medium. After 5 minutes the PMA2-GFP signal was measured on the apical and lateral side of the PM as well as the intracellular signal. No differences between the treatments were observed, an univariate ANOVA followed by a Tukey post-hoc was used. N = 32 cells from 2 biological replicates.



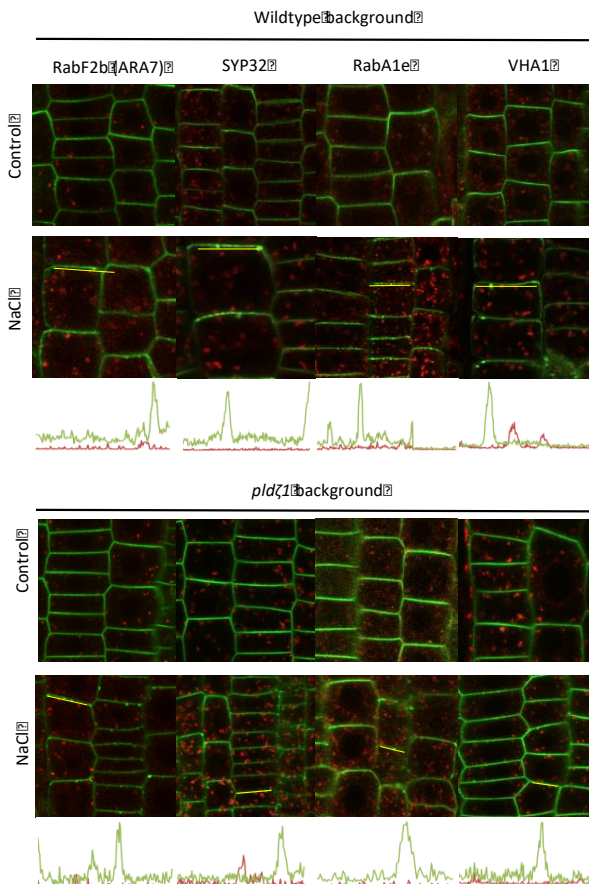
**Supplemental figure S4: Comparison of default, non-halotropic simulated auxin patterns in wildtype and *pldζ1* plants.** (A) Epidermal auxin levels as a function of distance from the root tip in wildtype and *pldζ1* plants. (B) Model PIN pattern, highlighting differences between wildtype and *pldζ1* in PIN2 patterning under both baseline conditions and salt stress. (C) Simulated DR5 auxin marker pattern for wildtype and *pldζ1* plants. Colors depict auxin concentration.



**Supplemental figure S5: Impact of baseline differences and salt induced differences in PIN2 polarity during halotropism and spatial data wildtype vs *pldζ1* during halotropism.** (A) Changes in epidermal auxin levels when combining *pldζ1* type halotropic PIN2 patterning changes with different baseline PIN2 patterns, wildtype, *pldζ1* or hybrid combinations over the lower part of the root after 24 hours. For comparison purposes also the auxin dynamics in wildtype plants are shown. (B) Changes in auxin rerouting for the different settings. A colored cell has an auxin increase of at least 10% the different colors depict different times. (C) Changes in epidermal auxin levels when combining *pldζ1* baseline PIN2 patterns with different salt induced changes in PIN2 patterning, wildtype, *pldζ1* or hybrid combinations. For comparison purposes also the auxin dynamics in wildtype plants are shown over the lower part of the root after 24 hours. (D) Changes in epidermal auxin levels for *pldζ1* and wildtype plants over the lower part of the root during halotropism after 24 hours.



**Supplemental figure S6: Sorbitol induces OSIMS similar to NaCl.** (A) Representative pictures of PIN2-GFP sub-cellular localization after 5 or 60 minutes of 240mM Sorbitol treatment. Inlays show an enlargement of one cell. (B) Quantification of the average number of OSIM structures per cell after 5 and 60 minutes of 240mM Sorbitol treatment, salt treatment data is shown for comparison. No significant differences using a univariate ANOVA followed by a Tukey post-hoc test ( $p < 0.05$ ) were found for either time point.



**Supplemental Figure S7: OSIMS do not co-localize with known endosomal markers.**

Representative images showing PIN2-GFP in wildtype and *pld1* background in combination with either RabF2b-RFP (ARA7) for multi-vesicular bodies, SYP32-RFP for the golgi network, RabA1e-RFP for recycling endosomes and VHA1-RFP for early endosomes after 5 minutes of salt stress. Yellow lines are the lines used for the profile plot through the OSIMS. Green line shows PIN2-GFP signal and the red line shows the endosomal marker RFP signal. No OSIMS are found in control conditions so no profile plots are shown.